Hydrothermal monitoring in a quiescent volcanic arc: Cascade Range, northwestern United States

S. E. INGEBRITSEN[1], N. G. RANDOLPH-FLAGG[1,2], K. D. GELWICK[1,3], E. A. LUNDSTROM[1,4], I. M. CRANKSHAW[1,5], A. M. MURVEIT[1,6], M. E. SCHMIDT[1,7], D. BERGFELD[1], K. R. SPICER[8], D. S. TUCKER[9], R. H. MARINER[1] AND W. C. EVANS[1]

[1]U.S. Geological Survey, Menlo Park, CA, USA; [2]Department of Earth and Planetary Science, University of California, Berkeley, CA, USA; [3]Department of Geology, Oberlin College, Oberlin, OH, USA; [4]Department of Geosciences, Princeton University, Princeton, NJ, USA; [5]Department of Geology, Carleton College, Northfield, MN, USA; [6]Department of Geology, Whitman College, Walla Walla, WA, USA; [7]Department of Earth Sciences, Brock University, St. Catharines, ON, Canada; [8]U.S. Geological Survey, Vancouver, WA, USA; [9]Mount Baker Volcano Research Center, Bellingham, WA, USA

ABSTRACT

Ongoing (1996–present) volcanic unrest near South Sister, Oregon, is accompanied by a striking set of hydrothermal anomalies, including elevated temperatures, elevated major ion concentrations, and $^3He/^4He$ ratios as large as 8.6 R_A in slightly thermal springs. These observations prompted the US Geological Survey to begin a systematic hydrothermal-monitoring effort encompassing 25 sites and 10 of the highest-risk volcanoes in the Cascade volcanic arc, from Mount Baker near the Canadian border to Lassen Peak in northern California. A concerted effort was made to develop hourly, multiyear records of temperature and/or hydrothermal solute flux, suitable for retrospective comparison with other continuous geophysical monitoring data. Targets included summit fumarole groups and springs/streams that show clear evidence of magmatic influence in the form of high $^3He/^4He$ ratios and/or anomalous fluxes of magmatic CO_2 or heat. As of 2009–2012, summit fumarole temperatures in the Cascade Range were generally near or below the local pure water boiling point; the maximum observed superheat was <2.5°C at Mount Baker. Variability in ground temperature records from the summit fumarole sites is temperature-dependent, with the hottest sites tending to show less variability. Seasonal variability in the hydrothermal solute flux from magmatically influenced springs varied from essentially undetectable to a factor of 5–10. This range of observed behavior owes mainly to the local climate regime, with strongly snow-melt-influenced springs and streams exhibiting more variability. As of the end of the 2012 field season, there had been 87 occurrences of local seismic energy densities approximately ≥ 0.001 J/m^3 during periods of hourly record. Hydrothermal responses to these small seismic stimuli were generally undetectable or ambiguous. Evaluation of multiyear to multidecadal trends indicates that whereas the hydrothermal system at Mount St. Helens is still fast-evolving in response to the 1980–present eruptive cycle, there is no clear evidence of ongoing long-term trends in hydrothermal activity at other Cascade Range volcanoes that have been active or restless during the past century (Baker, South Sister, and Lassen). Experience gained during the Cascade Range hydrothermal-monitoring experiment informs ongoing efforts to capture entire unrest cycles at more active but generally less accessible volcanoes such as those in the Aleutian arc.

Key words: heat flow, hydrothermal, noble gases, seismicity, volcano monitoring

Received 23 August 2013; accepted 16 January 2014

Corresponding author: Steve E. Ingebritsen, U.S. Geological Survey, Menlo Park, CA, USA.
Email: seingebr@usgs.gov. Tel: + 650-329-4422. Fax: + 650-329-4463.

INTRODUCTION

Time variation in hydrothermal phenomena can yield useful diagnostic information during volcanic unrest (e.g., Connor *et al.* 1993; Tedesco 1994; Chiodini *et al.* 2002;

Gottsmann *et al.* 2006, 2007; Todesco 2008; Todesco *et al.* 2010; Padron *et al.* 2013). However, most measurement and sampling of surficial hydrothermal features is carried out campaign-style, on a highly intermittent basis. Such intermittent data, with sampling frequencies often

≥ 1 year, are not well suited for comparison with continuous seismic and geodetic observations. Further, when volcanic unrest becomes evident from other geophysical data, baseline hydrothermal observations are sometimes nonexistent, and often limited to a few observations during the season when weather conditions are most amenable to field work. Finally, a preponderance of field season, daytime data means that there is limited information on seasonal or diurnal variability. Assuming that periodic variability is potentially significant, it is useful to establish a year-round data baseline in order to isolate anomalous changes.

Beginning in 2009, motivated by the dramatic hydrothermal anomalies associated with volcanic unrest at South Sister volcano (Wicks *et al.* 2002; Evans *et al.* 2004), the USGS made a concerted effort to develop hourly, multi-year hydrothermal records in the US portion of the Cascade Range, a 1200-km-long volcanic arc that extends from southern British Columbia to northern California. The 25 selected monitoring sites (Fig. 1) show evidence of magmatic influence in the form of high $^3He/^4He$ ratios and/or large fluxes of magmatic CO_2 or heat (Table 1).
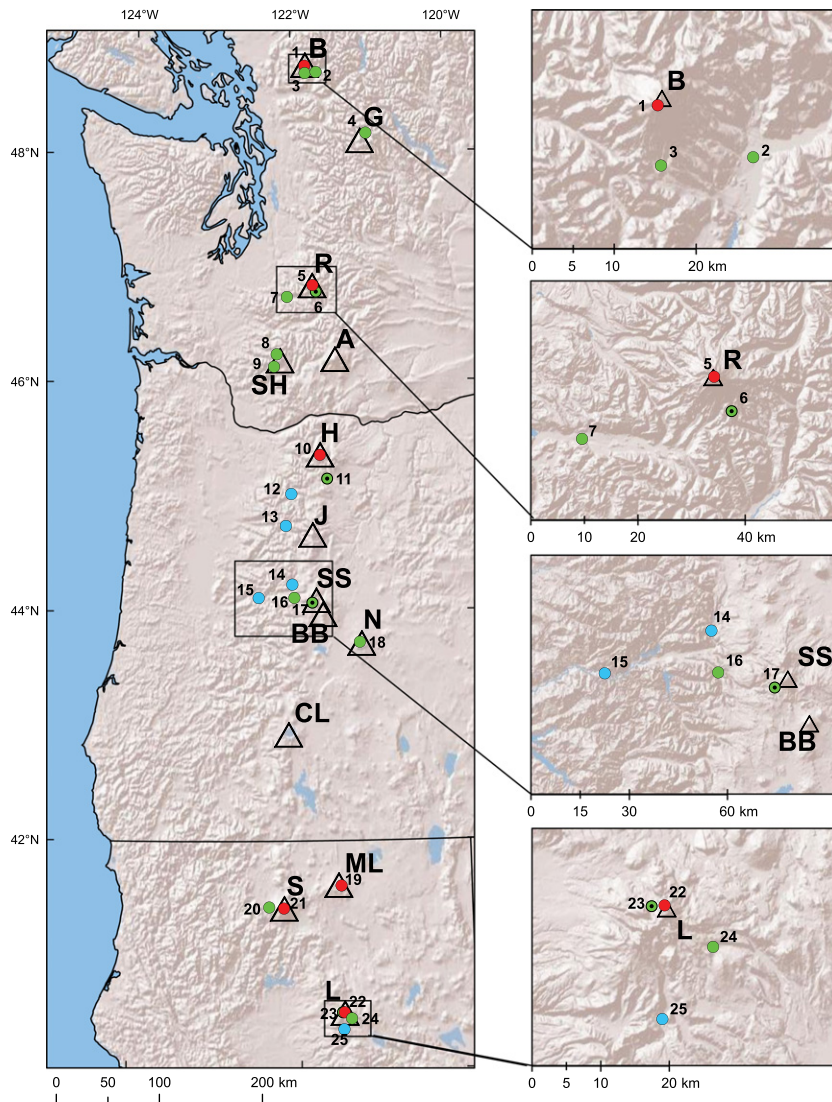

Fig. 1. Map of hydrothermal-monitoring sites in the US portion of the Cascade Range, numbered consecutively from north to south. Volcanoes (open triangles) are B, Mount Baker, G, Glacier Peak, R, Mount Rainier, A, Mount Adams, SH, Mount St. Helens, H, Mount Hood, J, Mount Jefferson, SS, South Sister, BB, Bachelor Butte, N, Newberry, CL, Crater Lake, ML, Medicine Lake, S, Mount Shasta, and L, Lassen Peak. Red circles denote sites with continuous temperature monitoring and intermittent gas sampling. Green circles denote sites with continuous pressure–temperature–conductivity monitoring and intermittent liquid sampling and discharge measurements; black dots within green circles indicate the availability of complementary vent temperature records. Blue circles indicate intermittent solute flux measurements extending over a period of several decades.

Table 1 Site summary.

Site no.	Volcano	Site name	Evidence of magmatic influence	Primary location(s)	Period of record	Measurement frequency	n	Primary variable	Mean value	SD
1	Baker	Sherman Crater	$^3He/^4He$ up to 7.7 R_A	48°46'11.1" 121°49'10.2"	2012-	Hourly		T*		
2	Baker	Boulder Cr.	Sherman Crater outflow	48°42'59.4" 121°41'38.5"	1975–2012	Intermittent	5	SO_4^{2-} flux	160 $g\,s^{-1}$	67
3	Baker	Sulphur Cr. trib.	>90% premodern carbon	48°42'24.8" 121°48'57.0"	2009–2012	Hourly	24 687	Cl^- flux	1.38 $g\,s^{-1}$	0.59
4	Glacier Peak	Gamma Cr.	Gamma Hot Sprs. outflow	48°10'29.8" 121°02'22.8"	1988–2011	Intermittent	7	Cl^- flux	4.4 $g\,s^{-1}$	1.5
5	Rainier	Summit	Approximately 10 MW heat discharge from summit fumaroles	46°51'14.2" 121°45'28.4"	2011–2012	Hourly	9888	T*	60.29°C	2.95
6	Rainier	Paradise Cr.	Paradise Warm Sprs. (1.9 R_A) outflow	46°47'43.4" 121°43'08.2"	2010–2012	Hourly	18 264	Cl^- flux	1.04 $g\,s^{-1}$	0.77
7	Rainier	Nisqually R.	Paradise Creek (etc.) outflow	46°45'08.9" 122°05'01.3"	2010–2012	Hourly	19 905	Cl^- flux	55.5 $g\,s^{-1}$	21.7
8	St. Helens	Carbonate springs	$^3He/^4He$ up to 1.9 R_A	46°15'10.3" 122°13'15.3"	2009–2012	Hourly	25 964	Cl^- flux	1.70 $g\,s^{-1}$	0.87
9	St. Helens	Kalama Spr.	Approximately 10% premodern carbon	46°08'39.7" 122°15'24.5"	2009–2012	Hourly	27 864	Cl^- flux	1.24 $g\,s^{-1}$	0.52
10	Hood	Crater Rock	$^3He/^4He$ up to 7.6 R_A	45°22'16.5" 121°41'59.4"	2010–2012	Hourly	12 042	T*	69.18°C	13.93
11	Hood	Still Cr.	Swim Warm Sprs. (7.2 R_A) outflow	45°17'36.9" 121°44'21.9"	2009–2012	Hourly	27 698	Cl^- flux	0.88 $g\,s^{-1}$	0.17
12		Austin Hot Sprs.	$^3He/^4He$ up to 5.7 R_A	45°07'29" 122°04'24"	1984–2006	Intermittent	30	Cl^- flux†	39.0 $g\,s^{-1}$	5.1
				45°07'29" 122°04'24"	2003–2006	Bi-daily to hourly	4405	Cl^- flux†	41.3 $g\,s^{-1}$	6.7
13		Breitenbush Hot Sprs.	$^3He/^4He$ up to 6.5 R_A	44°45'09.4" 122°07'44.3"	1984–2006	Intermittent	24	Cl^- flux†	15.6 $g\,s^{-1}$	1.6
14 and 15		McKenzie R.	Separation Cr. (etc.) outflow	44°14'21.6" 122°03'30.5" 44°07'30" 122°28'10"	1984–2012	Intermittent	82	Cl^- flux†	44.9 $g\,s^{-1}$	10.7
16	South Sister	Separation Cr.	Mesa Cr. (etc.) outflow	44°07'25.3" 122°02'03.7"	2002–2004	4-daily to hourly	21 465	Cl^- flux	10.0 $g\,s^{-1}$	0.62
					2006–2012		37 169		10.3 $g\,s^{-1}$	1.4
17	South Sister	Mesa Cr.	Mesa Sprs. (up to 8.6 R_A) outflow	44°04'48.9" 121°49'11.9"	2002–2007	Bi-daily to hourly	5693	Cl^- flux†	0.175 $g\,s^{-1}$	0.029
					2008–2012		34 870		0.229 $g\,s^{-1}$	0.042
18	Newberry	Paulina hot sprs.	$^3He/^4He$ up to 8.0 R_A	43°43'54.6" 121°15'04.7"	1993–2012	Intermittent	10	T*	57.3°C	0.6
19	Medicine L.	Hot Spot	$^3He/^4He$ up to 2.1 R_A	41°36'18.8" 121°31'26.0"	2011–2012	Hourly	6317	T*	58.1°C	18.3
20	Shasta	Summit	$^3He/^4He$ up to 6.2 R_A	41°24'34.4" 122°11'46.1"	2011–2012	Hourly	8016	T*	82.14°C	0.40
21	Shasta	Boles Cr.	$^3He/^4He$ up to 6.9 R_A	41°21'11.5" 122°22'06.2"	2007–2012	Hourly	44 992	Cl^- flux	0.149 $g\,s^{-1}$	0.006
22	Lassen	N flank Lassen Peak	T up to 90.5°C, >50% CO_2 in dry gas	40°29'47.5" 121°30'41.6"	2010–2012	Hourly	14 686	T*	83.48°C	3.78
23	Lassen	Manzanita Cr. trib.	98.5% premodern carbon, $^3He/^4He$ up to 1.8 R_A	40°29'49.5" 121°32'09.1"	2009–2010	Hourly	28 220	HCO_3^- flux	3.2 $g\,s^{-1}$	1.2

Table 1. (Continued)

Site no.	Volcano	Site name	Evidence of magmatic influence	Primary location(s)	Period of record	Measurement frequency	n	Primary variable	Mean value	SD
24	Lassen	Devils Kitchen	^{3}He/^{4}He up to 7.3 R_A in Lassen fumaroles	40°26′26.5″ 121°25′45.5″	1922–1996 2010–2012	Intermittent Hourly	15 17 616	Heat flux Heat flux	13.5 MW 10.9 MW	4.5 4.4
25	Lassen	Mill Cr.	Lassen-sourced high-Cl⁻ hot spring outflow	40°20′49.5″ 121°31′07.8″	1983–2012	Intermittent	48	Cl⁻ flux†	42.5 g s⁻¹	5.1

*Temperature (T) was typically monitored at 3–6 points at those sites where it was the primary variable. Mean ± SD values shown in this summary table are from the hottest points that possess a minimum of 6 months of continuous record.†The chloride (Cl⁻) flux values for these sites represent the hydrothermal component only; that is, the background Cl⁻ values upstream of the hydrothermal sources have been subtracted from the downstream Cl⁻ values (Fig. 4). Other Cl⁻ flux values are total fluxes for those sites where no effort was made to identify and correct for background (nonhydrothermal) Cl⁻.

Hydrothermal anomalies associated with volcanic unrest at South Sister

Geodetic deformation centered about 5 km west of the summit of South Sister, Oregon, began in 1996–1997 and was first recognized in 2001 (Wicks *et al.* 2002). The center of geodetic uplift coincides with elevated water temperatures, elevated chloride (Cl⁻) and sulfate (SO_4^{2-}) concentrations, and elevated ^{3}He/^{4}He ratios observed in numerous springs. Spring temperatures exceed local ambient by as much as 5°C; Cl⁻ and SO_4^{2-} concentrations exceed local ambient by as much as a factor of 40; and maximum ^{3}He/^{4}He ratios (up to $8.6R_A$) are the highest ever sampled in the Cascade or Aleutian volcanic arcs (Evans *et al.* 2002, 2004). The geochemical anomalies coincide almost perfectly with the center of geodetic uplift (Fig. 2). A strong correlation between chloride concentration and temperature within individual spring groups (Evans *et al.* 2004; their Fig. 2C), the observation that all helium–isotope ratios >$4R_A$ occur in springs with anomalous chloride, and a strong regional correlation between Cl⁻ and ^{3}He concentrations (Fig. 3) combine to suggest that the source of anomalous heat and solutes is magmatic; further, magmatic carbon (δ^{13}C approximately −9‰) predominates in most of the springs (Evans *et al.* 2004). The resulting conceptual model for the hydrothermal system under the western flank of South Sister, based in part on the observation that the sulfate-enriched springs are generally upslope of the chloride-enriched springs (Fig. 2, upper panel), is similar to that invoked for other, more visible hydrothermal systems, including phase separation, scrubbing, and lateral outflow of brines (Iverson 1999; Evans *et al.* 2004).

In addition to the well-documented hydrothermal anomaly associated with unrest at South Sister, there is an anecdotal report that the temperature and discharge of Loowit springs at Mount St. Helens increased prior to the renewal of the eruption in 2004: 'Just prior to the onset of seismicity in 2004, discharge and water temperature at a spring in Loowit canyon appeared higher than normal (J.S. Pallister, USGS, oral communication, 2004), but no measurements were made…' (Bergfeld *et al.* 2008).

A regional hydrothermal-monitoring network

Both at South Sister and at Mount St. Helens, there are few (if any) hydrothermal-monitoring data that span the entire period of unrest. Indeed, this is typically the case. Hydrothermal sampling campaigns are usually prompted by other geophysical indications of unrest (e.g., seismic or geodetic). The resulting data are often sparse, lacking adequate context to permit confident interpretation. Further, even in the absence of unrest, many hydrothermal signals seem likely to exhibit substantial periodic variability (seasonal, diurnal) (e.g., Ingebritsen *et al.* 2001). Such
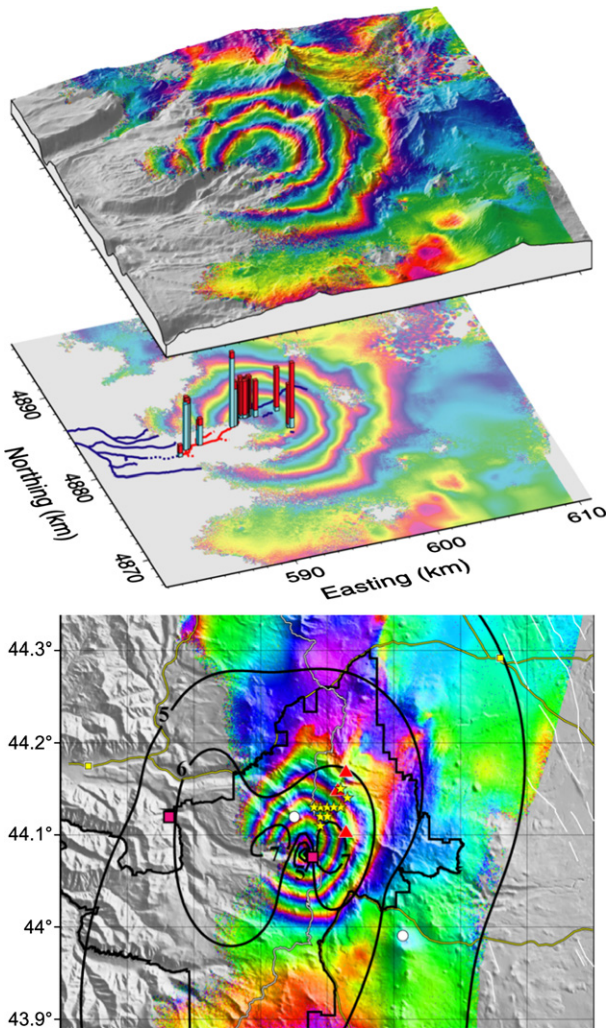
Fig. 2. Upper panels: South Sister location map showing 1996–2004 InSAR interferogram (one color cycle = 2.83 cm) and geochemical data: blue columns indicate chloride concentrations (0.6–18.6 mg l⁻¹ versus a regional background of 0.2–0.7 mg l⁻¹) and red columns indicate SO_4^{2-}/Cl^- ratios (range 0.2 to 2.8). Lower panel: Locations of monitoring sites (16) and (17) of this study (pink squares) and contoured ^3He/^4He ratio in springs. Red triangles are the Three Sisters; yellow stars are epicenters of earthquakes on March 23, 2004; open circles are continuous GPS stations; and yellow squares are the communities of McKenzie Bridge (west) and Sisters (east). From Wicks *et al.* (2002) and C.W. Wicks, Jr., USGS, written communication, 2004; He–isotope contours for Cl^--enriched springs are based on the data of Evans and others (2004, their Fig. 1).

variability must be documented and understood to discern the potentially anomalous behaviors that we are ultimately interested in.

Signs of volcanic unrest (Wicks *et al.* 2002) and the associated geochemical anomaly (Iverson 1999; Evans *et al.* 2002, 2004) prompted a concerted hydrothermal-monitoring effort at South Sister and a few other Cascade Range sites beginning in 2002. In 2009–2012, this monitoring network was expanded to include 25 sites that quantify baseline hydrothermal variability at most (10 of 12) of the
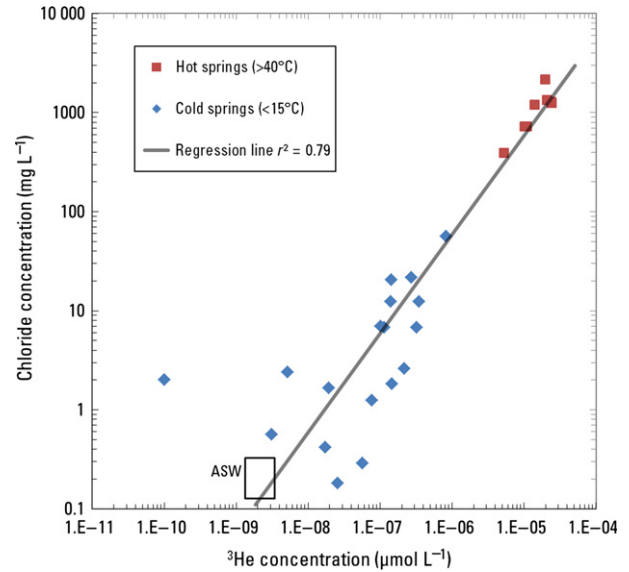

Fig. 3. Relation between chloride and ^3He concentration for cold to slightly thermal springs in the Three Sisters area and hot springs in the Oregon Cascades. From van Soest *et al.* (2004).

highest-risk volcanoes in the Cascades, as defined by the US Geological Survey's (USGS) National Volcano Early Warning System (NVEWS) report (Ewert *et al.* 2005).

The 25 monitoring sites can be grouped into three broad categories (Fig. 1): (i) sites with hourly pressure–temperature–conductivity monitoring and intermittent liquid sampling and discharge measurements, in some instances with complementary temperature records from a nearby source vent; (ii) sites with hourly temperature monitoring and intermittent gas sampling; and (iii) sites that lack hourly data, but where the USGS has carried out intermittent solute flux measurements over a period of several decades.

Accompanying USGS Data Set

A USGS data set that accompanies this paper (Ingebritsen *et al.* 2014) includes 24 workbook files for the monitoring sites shown in Fig. 1 (sites 14 and 15 are combined in one workbook file). The USGS data set includes the full instrumental time series, so that potential users can choose which data to omit, filter, or correct. The only embedded corrections are the handful of known depth offsets described in the workbook files. In addition to hourly measurement records, the workbook files include records of all field measurements, sampling, and analytical results; 'rating curve' information such as correlations between water depth and steam discharge; and relevant published and unpublished historical data (e.g., water and gas chemistry). The USGS data set also includes metadata and background for each of the 25 sites and, like the site numbers, is ordered consecutively north to south.

Purpose and scope

The primary objectives of this paper were to generally introduce the available Cascade Range hydrothermal data and to carry out some basic analysis with a focus on seasonal and diurnal variability, seismic response, and long-term trends at selected sites. Detailed time-series analysis is intended to be the subject of a future paper.

METHODS

Hydrothermal phenomena were monitored at 25 sites from Mount Baker in the north to the Lassen volcanic center in the south (Fig. 1). As described in Table 1 and in the USGS data set that complements this paper, all 25 sites have some indication of magmatic influence, such as elevated $^3He/^4He$ ratios, large fluxes of magmatic CO_2, or large heat fluxes.

At 14 of the sites, pressure, temperature, and electrical conductivity (P-T-C) were measured on an hourly basis. At six sites – mainly summit fumarole sites – hourly temperature (T-only) measurements were complemented by intermittent gas sampling. The other five sites have limited hourly data, but each has a several-decade history of intermittent solute flux measurement. Records of hourly data in the South Sister area (sites 16 and 17) begin in 2002, in response to the volcanic unrest (Wicks *et al.* 2002), but most of the hourly data were recorded in 2009–present.

Solute inventory methods (Ellis & Wilson 1955; Ingebritsen *et al.* 2001) were used to convert P-T-C records to solute flux records (Fig. 4). In most cases, the solute of interest was chloride (Cl^-) because, in the young volcanic rocks of the Cascade Range, elevated Cl^- levels invariably indicate a contribution of deep, hydrothermal fluid. In the absence of deep contributions, Cl^- levels tend to be in the range of local precipitation (0.2–0.6 mg l^{-1}; Ingebritsen *et al.* 1994). Chloride behaves conservatively in solution, so that fluxes can be reliably measured far downstream from the actual source. At a few of the sites, however, fluxes of SO_4^{2-}, HCO_3^-, or heat (rather than Cl^-) are the quantities of interest.

For most sites, correlations have been developed to convert pressure–temperature–conductivity data into a flux of heat or (more often) to the flux of a solute species of interest. Correlations have been used to relate (i) specific conductance to laboratory-measured concentrations of dissolved constituents (e.g., Fig. 5A) and (ii) pressure (depth) to field-measured discharge (e.g., Fig. 5B).
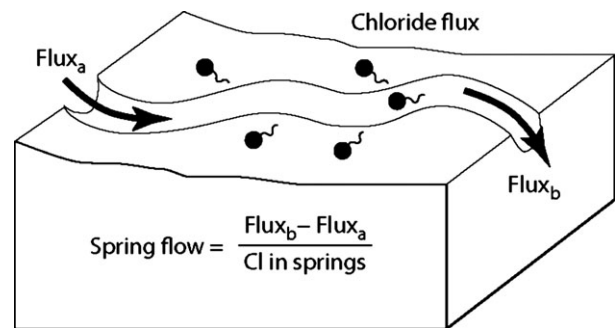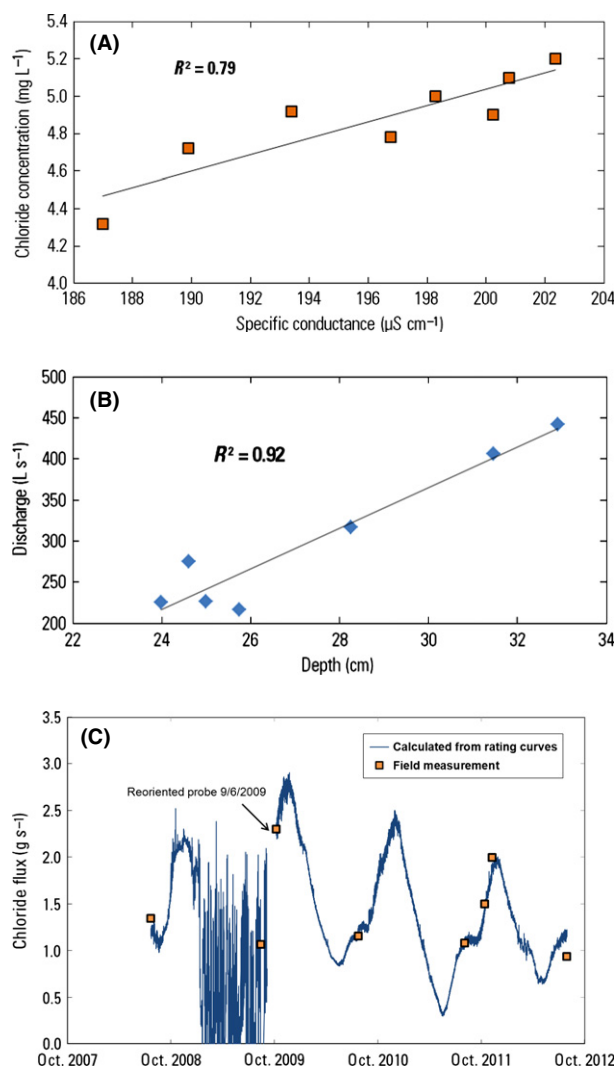

Fig. 4. Block diagram illustrating solute inventory method for the case of chloride. The difference between chloride flux upstream (Flux$_a$, g s^{-1}) and downstream (Flux$_b$) of a thermal spring group is divided by the chloride concentration in the thermal spring waters (g l^{-1}) to determine thermal spring discharge (l s^{-1}). That is, $D_{ts} \sim (D_s[Cl_d-Cl_u]/Cl_t)$, assuming that $D_{ts} \ll D_s$ and $Cl_t \gg Cl_d$ or Cl_u, where D_{ts} is thermal spring discharge, D_s is stream discharge, Cl_d and Cl_u are stream chloride concentrations below and above the thermal springs, respectively, and Cl_t is chloride concentration in the thermal springs themselves.

Fig. 5. Data from an unnamed tributary of Sulphur Creek with >90% pre-modern carbon (site 3), showing how instrumental P-T-C records are converted to solute flux time series: Rating curves relating (A) chloride concentration to specific conductance and (B) depth to discharge, and (C) resulting hourly flux estimates compared with discrete field measurements.

Field methods

Most of the pressure, temperature, and electrical conductivity (P-T-C) records were developed using Aqua TROLL 200 instruments (In Situ Inc.). Insofar as practical, the P-T-C probes were deployed subhorizontally, entirely submerged and anchored securely to the streambed with lengths of rebar. During field visits, stored P-T-C data from the probes were downloaded to portable computers, and a field check of the probe data was made using laboratory-calibrated meters (T and C) and tape-down measurements of water level relative to a standard measuring point (P).

Except in the rare instances where P-T-C probes were collocated with USGS streamgaging stations, stream discharge was measured during each field visit by standard wading methods (Nolan & Shields 2000) in order to develop a rating curve to convert depth (P) records to discharge records. Water samples were collected within about 1 m of the P-T-C probes to create empirical relations between electrical conductivity (specific conductance, C) and concentrations of the ionic species of interest (e.g., Fig. 5A). Samples were collected using a syringe pump with a 0.45-µm membrane filter. Two 30- or 60-ml splits of the filtered water were retained for chemical analyses, including an unacidified (FU) sample for the determination of anion concentrations and a nitric acid-preserved (FA; 1% v/v concentrated trace metal grade HNO_3) sample for cation and trace metal analyses.

Hourly temperature (T-only) records were developed mainly for summit fumarole sites (Fig. 1). These records were developed using HOBO U12-015-02 and HOBO Pro v2 sensors. The sensors – typically 3–6 sensors per site – were buried tens of cm deep in heated ground. During field visits, temperature profiles were measured at 2- to 10-cm-depth intervals to approximately 50 cm depth at each sensor point. The summit sites are difficult to access and often inclement, and their high-temperature, low-pH conditions are hostile to instrumentation. Thus, the onsite instruments were swapped out annually, and data were downloaded offsite, rather than in the field. At 4 of the P-T-C sites, complementary T-only records of upstream vent conditions were developed using HOBO Pro v2 and Tidbit sensors.

At both the P-T-C and T-only monitoring sites, water and/or gas samples were collected, including samples for noble gas analyses, using standard methods. Gas samples for bulk composition and $\delta^{13}C$–CO_2 analyses were collected into pre-evacuated glass bottles through a titanium tube (from gas vents) or a funnel fitted with Tygon tubing (from bubbling springs). Prior to sampling, each collection system was purged of atmospheric gases. Most gas samples for $^3He/^4He$ analysis were collected through a titanium rod (from gas vents) or a funnel and tubing apparatus (from springs) into copper tubing that was then sealed at both ends with refrigeration clamps.

Laboratory methods

Concentrations of anions (chloride, fluoride, bromide, and sulfate) were determined with a Dionex ion chromatograph ICS-2000 at the USGS in Menlo Park, California. Analytical errors for these constituents are typically <5%. Total alkalinity as bicarbonate was determined either in the field with a HACH digital pipet or in the laboratory with a calibrated syringe pump titrator (Barringer & Johnsson 1996); sample aliquots were titrated with standardized sulfuric acid to the bicarbonate end point. The analytical error in alkalinity concentrations is <5%. Concentrations of major cations and trace metals were determined using inductively coupled plasma–optical emission spectrometry at the USGS in Menlo Park. Several techniques were used to assure the quality of these analytical data, including analysis of USGS standard reference water samples (SRWS) and replicate determinations in the laboratory. Gas samples were analyzed for bulk composition at the USGS in Menlo Park using gas chromatography methods reported in Evans *et al.* (1981). Carbon dioxide for stable isotope analysis was separated from the bulk gas sample using standard cryogenic techniques on a vacuum line (Evans *et al.* 2002, 2004); the isotopic analyses were carried out at the USGS laboratories in Reston, Virginia. The $^3He/^4He$ determinations were performed at Lawrence Berkeley National Laboratory in Berkeley, California (Kennedy *et al.* 1985; Hiyagon & Kennedy 1992), the USGS laboratories in Denver, Colorado, and the University of Utah Noble Gas Laboratory.

Data quality

The accuracy of field measurements and analytical results reported here is consistent with the number of significant digits assigned. The accuracy of the instrumental P-T-C time series is variable and best judged by comparison with complementary field measurements and analytical results. Pressure (depth) records are the most likely to contain spurious values. For instance, the flux records from sites (3), (9), and (20) include discrete periods of oscillation that are undoubtedly nonphysical and owe to oscillations in the pressure record (e.g., Fig. 5C). Nearly all of the pressure transducers used in this study were connected to the local atmosphere through a vented cable, and most periods of pressure oscillation likely reflect disrupted venting (clogged or punctured venting tubes). Conductivity drift affects a few of the flux records, most notably that from site (8). The temperature records are generally reliable (i.e., within errors cited by the manufacturers). Although all of the temperature sensors that we used were vulnerable to failure under high-temperature (approximately ≥70°C), low-pH conditions, the failures tended to be abrupt, such that the surviving records appear accurate. The only clear instance of prefailure thermistor drift is from site (22).

PERIODIC VARIABILITY OF THE HYDROTHERMAL SIGNALS

Many of the hydrothermal signals exhibit substantial periodic variability (seasonal, diurnal). Because the onset of volcanic unrest is not restricted to the traditional field season, it is useful to document and understand this variability. Thus, a primary goal of this study was to develop and interpret multiyear time series sampled with hourly frequency, sufficient to evaluate seasonal to subdiurnal variability. In this section, we consider hourly temperature (T-only) records from 6 summit fumarole sites, hourly solute fluxes (e.g., Fig. 5) from 14 P-T-C sites, and spring vent temperature records from selected sites.

Temperature records from summit fumarole sites

Thermistor profiles at the six summit fumarole sites span areas of near-boiling ground temperature (Fig. 6) and were designed to capture horizontal gradients in temperature and heat flow. We experienced a fair amount of instrument failure under high-temperature ($\geq 70°C$) low-pH conditions, despite using instruments nominally rated to at least $105°C$ for the hotter ($50–90°C$) points. However, by the end of the 2012 field season, we had obtained a total of 26 records ≥ 6 months in length from five different summit fumarole sites (Table 2).

Both visual (Fig. 7) and statistical (Fig. 8) assessments indicate that the higher-temperature records are generally less variable than the lower-temperature records. The coefficient of variation (CV; mean/standard deviation) is one measure of variability in relation to the mean, and about 2/3 of the CV

variation seen in the 26 longer (>6 month) records is explained by variance in the mean temperature (Fig. 8).

The experimental design (Fig. 6) was based on the premise that variability in temperature would tend to be greater on the flanks of local thermal anomalies than in the heart of the anomaly. Measurements were taken along a horizontal transect to capture a gradient across a local anomaly. Near-boiling ground temperatures must be supported by vigorous upflow of water vapor, and such upflow will tend to inhibit the influence of surface environmental parameters (air temperature, snowmelt, and atmospheric pressure) that drives much of the observed variability at lower-temperature points (Fig. 7). Previous field measurements at various sites with near-boiling ground temperatures indicate total heat flux values on the order of 2 kW m^{-2} (Hochstein & Bromley 2005). If this heat flux is supported by saturated water vapor of maximum enthalpy (2804 J g^{-1}), the corresponding vapor upflow rates are on the order of $1 \text{ g s}^{-1} \text{ m}^{-2}$. Ground temperatures of $25–30°C$ imply heat fluxes (and vapor upflow rates) about 10 times smaller (Hochstein & Bromley 2005).

As of 2009–2012, summit fumarole temperatures in the Cascade Range were generally at or below the local boiling temperature, indicating substantial interaction with meteoric water. Maximum observed temperatures were slightly in excess of the local pure water boiling point at Mount Baker ($+2.4°C$), Mount Hood ($+0.5°C$), Mount Shasta ($+0.6°C$), and the north flank of Lassen Peak ($+0.8°C$) (Table 2). In light of stated instrumental accuracy of $\pm 0.7°C$ at $90°C$ plus positive drift of $0.1°C$ per 1000 h of use at $100°C$ (http://www.onsetcomp.com/products/
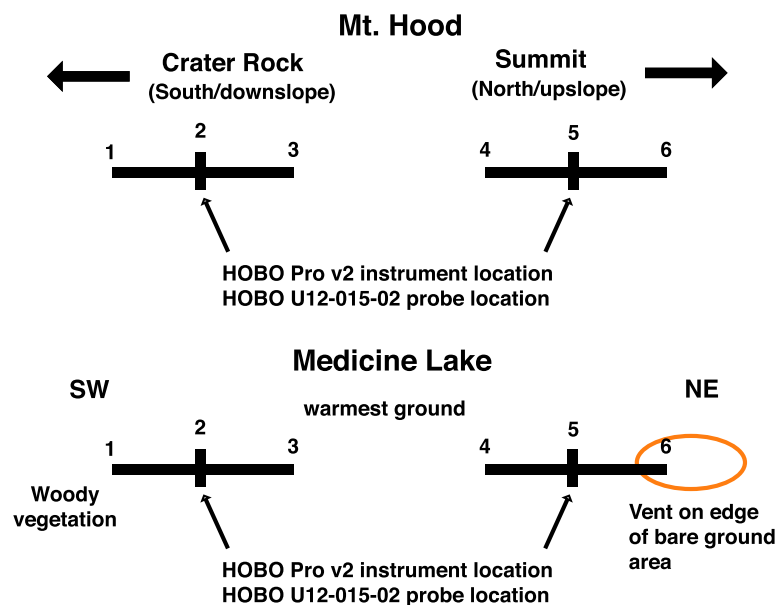

Fig. 6. Schematic diagrams illustrating temperature sensor configurations in the fumarolic area near Crater Rock, Mount Hood (upper panel) and at the Medicine Lake Hot Spot (lower panel). Point numbers correspond to those in Table 2. The two thermistor profiles shown in the upper panel (points 1–3 and 4–6) each span approximately 2.5 m and are about 30 m apart. The single thermistor profile shown in the lower panel (points 1–6) spans approximately 4 m.

Table 2 Summary of temperature (^{o}C) records from summit-fumarole sites

Site no.	Volcano/Site Name	Elev. (m)	Boilingpoint*	Max. meas'd. temp.	Point no.	Period of record	Mean(SD)[†] temperature
1	Baker/Sherman Crater	3002	89.4	91.8	(1)	–	–
					(2)	–	–
					(3)	–	–
5	Rainier/Summit	4350	85.3	64.9	(1)	07/06/11–08/21/12	60.29 (2.95)
					(2)	07/06/11–08/21/12	53.62 (3.62)
					(3)	07/06/11–09/28/11	–
					Cntrl.[‡]	07/06/11–08/21/12	5.66 (9.66)
10	Hood/Crater Rock	3189	89.1	88.9	(1)	07/17/09–07/23/09	–
						07/09/11–07/21/11	–
					(2)	10/16/10–03/01/12	69.18 (13.8)
					(3)	07/17/09–07/23/09	–
						07/09/11–07/25/11	–
					(4)	10/16/10–11/05/10	–
						07/09/11–07/21/11	–
					(5)	10/16/10–07/28/11	63.72 (18.2)
					(6)	10/16/10–11/06/10	–
						11/07/10–07/16/11	83.93 (7.35)
19	Medicine Lake/Hot Spot	2146	92.6	83	(1)	06/23/09–06/17/10	15.82 (8.44)
						07/05/10–08/11/11	12.24 (8.96)
						08/11/11–07/11/12	22.56 (9.88)
					(2)	08/11/11–07/11/12	18.68 (9.00)
					(3)	06/23/09–06/17/10	26.34 (13.4)
						07/05/10–08/11/11	16.63 (11.8)
						08/11/11–07/11/12	12.66 (7.45)
					(4)	07/05/10–08/11/11	38.98 (10.8)
						08/11/11–04/30/12	58.08 (18.3)
					(5)	08/11/11–07/11/12	38.98 (10.8)
					(6)	07/05/10–08/11/11	34.11 (26.0)
						08/11/11–04/30/12	26.98 (10.6)
20	Shasta/Summit	4253	85.5	86.1	(1)	08/11/09–07/16/11	13.23 (5.96)
					(2)	08/11/09–07/16/11	31.90 (6.90)
					(3)	07/16/11–06/14/12	82.15 (0.40)
22	Lassen/N flank Lassen Peak	2781	90.7	91.5	(1)	07/13/09–11/24/09	–
						10/12/10–09/02/11	58.26 (3.81)
					(2)	07/13/09–11/24/09	–
						10/12/10–12/15/10	–
					(3)	10/12/10–06/15/12	83.48 (3.78)
					(4)	10/12/10–12/11/10	–
						09/02/11–01/23/12	–
					(5)	07/13/09–06/15/12	17.55 (8.46)
					Sun[‡]	10/12/10–06/15/12	7.34 (9.76)
					Shade[‡]	10/12/10–06/15/12	5.08 (7.07)

*Nominal pure-water boiling temperature at site elevation. †Calculated only for periods of continuous record >6 months.‡Ground temperature outside thermal anomaly.

data-loggers/u12-015-02), and the fact that the pressure changes associated with storm fronts can change the local boiling point by about 1°C, only the Mount Baker result clearly indicates some degree of superheat.

Much higher fumarole temperatures have been observed previously in the Cascade Range. For instance, during the California drought of 1976–1977, the temperature of Big Boiler fumarole at Lassen (2500 m elevation) reached 159°C, close to the temperature (163°C) of steam decompressed adiabatically from saturated steam of maximum enthalpy (2804 kJ kg^{-1}, 235°C) to Lassen surface pressure (0.75 bars) (Muffler *et al.* 1982). The large values of superheat at Lassen were recorded by campaign-style measurement. Because there are no continuous,

long-term fumarole temperature records in the Cascade Range, it is impossible to determine whether other drought periods have led to significant superheat. Fumarole temperatures > 163°C can only be achieved in the complete absence of liquid water, and such temperatures have been observed in the Cascade Range only in immediate aftermath of the 1980 eruption of Mount St. Helens (Evans *et al.* 1981).

Temperature records from spring vents

Although hourly temperature (T-only) records were developed mainly for summit fumarole sites (Table 2), complementary T-only records of upstream spring vent conditions
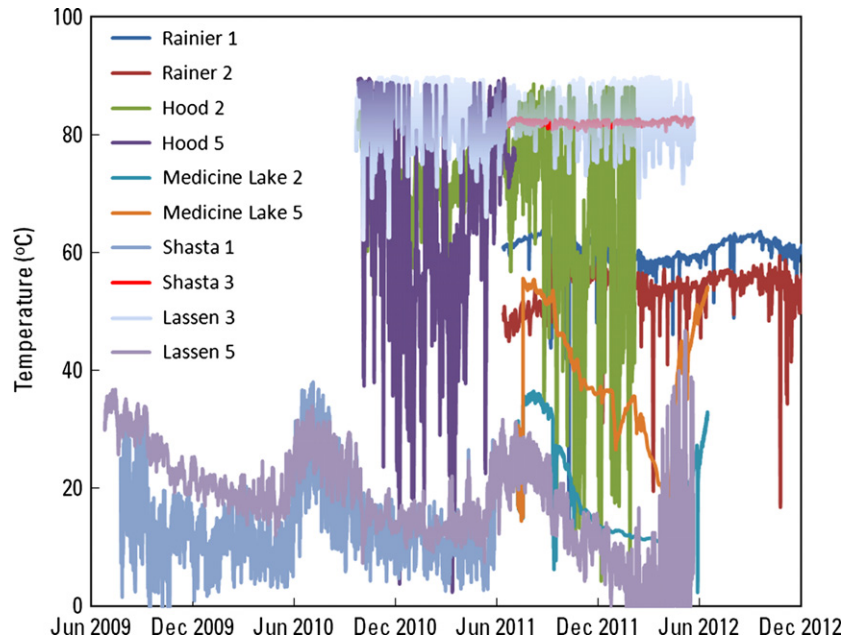
Fig. 7. Temperature records from selected summit fumarole sites – see Tables 1 and 2 for site information and Fig. 1 for locations.
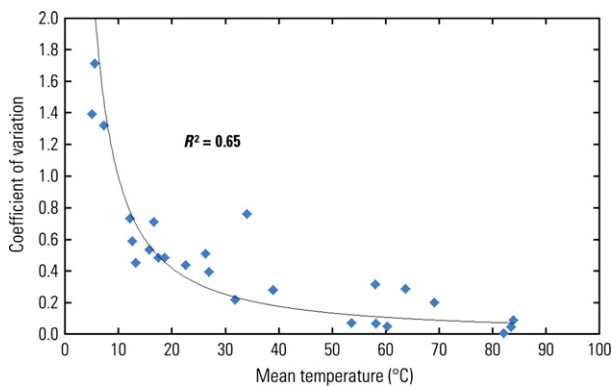

Fig. 8. Coefficient of variation (std. deviation/mean) as a function of mean temperature at summit fumarole sites (Table 2).

were developed for four of the P-T-C (solute flux) sites. The temperatures of these cold to slightly thermal springs were very stable over the period of observation (Fig. 9).

Whereas nearby air and ground temperatures vary annually by as much as 50°C, spring temperatures are nearly constant (typically $\pm$ 0.1°C). The only significant variations in spring vent temperature occur at Paradise Warm Springs, located at 1,934 m elevation on the south flank of Mount Rainer; there, where the mean temperature is approximately 22.5°C, episodic snowmelt causes excursions to temperatures as low as 17.4°C.

Solute flux records

At 14 of the 25 hydrothermal-monitoring sites, pressure, temperature, and electrical conductivity (P-T-C) were measured on an hourly basis and converted to solute flux records (e.g., Fig. 5). Each of these sites has some indication of magmatic influence such as elevated ^{3}He/^{4}He ratios, large fluxes of magmatic CO_2, or anomalous heat fluxes (Table 1). In most cases, the primary solute of
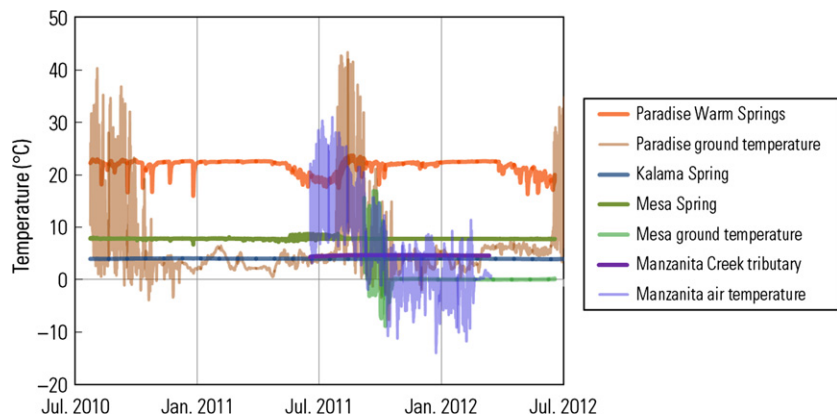
Fig. 9. Spring vent, ground, and air temperature records from selected sites (sites 5, 9, 17, and 23 – see Tables 1 and 3 for site information and Fig. 1 for locations).
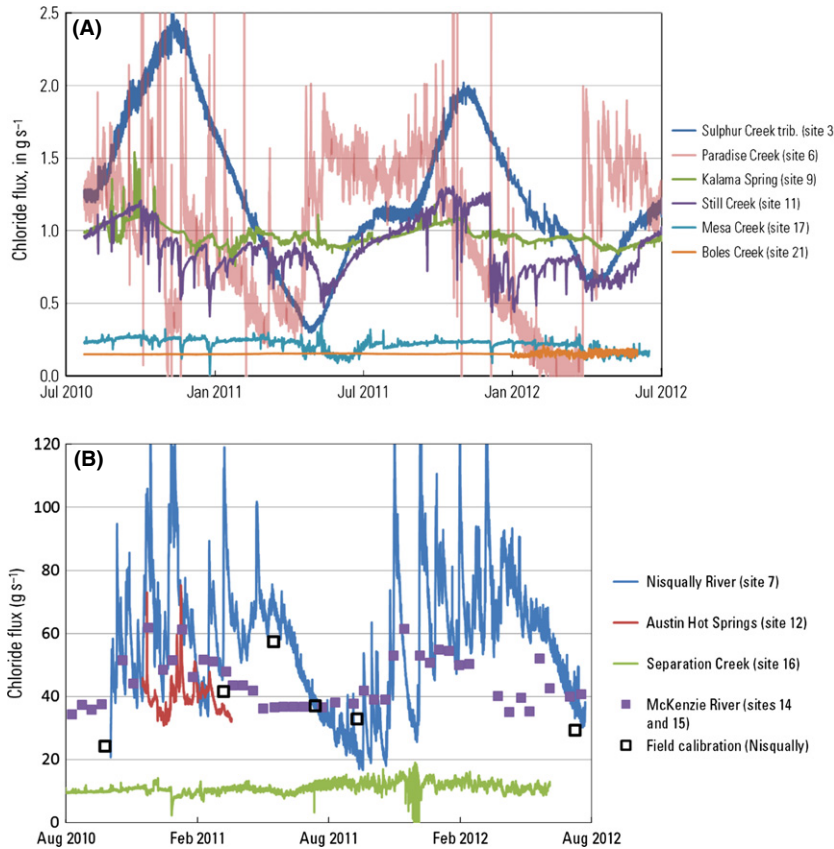
Fig. 10. Two-year time series of chloride flux in (A) smaller streams that capture outflow from nearby (≤400 m distant) springs with evidence of magmatic influence (sites 3, 6, 9, 11, 17, 21) and (B) larger streams with more remote hydrothermal input (sites 7, 12, 14–15, and 16). See Tables 1 and 3 for site information and Fig. 1 for locations. Austin Hot Springs (Clackamas River) data from 2003–2004 (site 12) and McKenzie River from 2002–2004 (sites 14 and 15) are transposed for comparison.

interest is chloride (Cl^-) because, in the Cascade Range, elevated Cl^- levels invariably indicate a contribution of deep, hydrothermal fluid. Further, in the Three Sisters area, Cl^- concentrations have been shown to be well correlated with ^3He concentrations (Fig. 3).

Figure 10 shows two-year chloride flux records from smaller streams that capture outflow from nearby springs with evidence of magmatic influence (Fig. 10A) and larger streams with more remote hydrothermal input (Fig. 10B). There is a wide range of variability. Among the smaller streams, seasonal variability in Cl^- flux ranges from essentially undetectable at Boles Creek in northern California (site 21) to a factor of 5–10 at Sulphur Creek tributary (site 3) and Paradise Creek (site 6) in Washington. Several of the larger streams (Fig. 10B) show a tendency toward larger solute fluxes in winter and spring, with lower fluxes in late summer and early fall.

The variability observed in the smaller streams (Fig. 10A) seems to owe largely to local climatic conditions. The most northerly of the small streams (Sulphur Cr. tributary and Paradise Cr.), which have the largest seasonal variability (Fig. 10A), also have the largest late-summer diurnal variability (Fig. 11). Large quantities of snow and ice are present year-round in the Paradise Creek watershed, and the late-summer diurnal variability there clearly owes to snowmelt. In contrast, snow cover is mini-

mal or absent nearly year-round at Boles Creek, located at 1091 m elevation on the northwest flank of Mount Shasta. Thus, the observed range of variability may reflect the general distinction between 'spring-fed' and 'snowmelt-fed' springs that was documented by Manga (1996, 1997) in the Oregon Cascades. In many instances, the observed variability in solute flux primarily reflects variability in discharge (Table 3), and the discharge of the 'snowmelt-fed' springs is much more variable.

As a partial test of this hypothesis, we can compare the observed variability in solute flux to some proxy for local climate conditions. Land-surface elevation serves as a crude proxy for climate in much of western North America. However, because our monitoring sites span more than 8 degrees of latitude (Fig. 1), latitude may be equally or more important. Linear regression of coefficient of variation for small streams versus site elevation yields an insignificant correlation (Fig. 12A). However, regression of CV versus an 'effective elevation' normalized to 45°N latitude seems to explain most of the variance in the data (Fig. 12B). Here, the 'effective elevation' of the monitoring sites was calculated on the basis of a wet adiabatic lapse rate of 5.4°C per km elevation (Ingebritsen *et al.* 1994, their Fig. 21) and the 0.9°C per degree latitude variation in mean annual air temperature typical of North America east of the Rocky Mountains (http://www.ncdc.noaa.
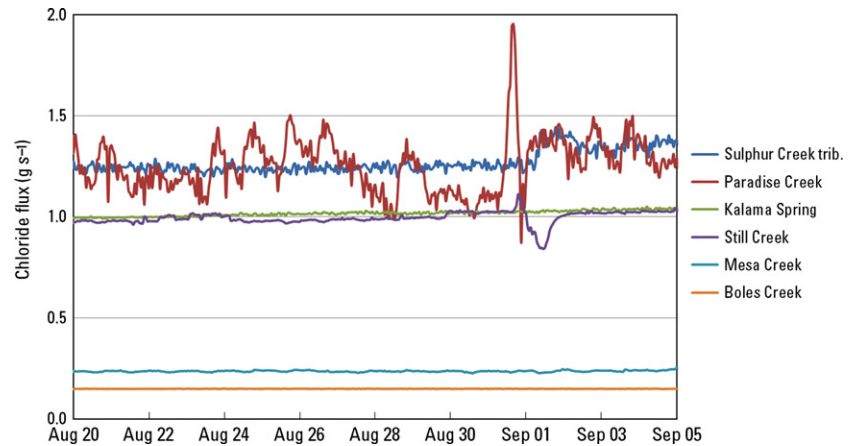
Fig. 11. Two-week late-summer (2011) time series of chloride flux in smaller streams that capture outflow from nearby (≤400 m distant) springs with the evidence of magmatic influence (sites 3, 6, 9, 11, 17, 21).

Table 3 Correlations (r^2 for linear regression) between measured fluxes, stream discharge, and concentration or ΔT.

Site no.	Volcano/Site name	Period of record	Measurement frequency	n	Primary variable	Correlation with discharge*	Correlation with concentration or ΔT*
2	Baker/Boulder Creek	1975–2012	Intermittent	5	SO_4^{2-} flux	0.04	0.31
3	Baker/Sulphur Creek trib.	10/09/09–08/02/12	Hourly	24 687	Cl^- flux	0.98	(0.08)
4	Glacier Peak/Gamma Creek	1988–2011	Intermittent	7	Cl^- flux	0.94	(0.90)
6	Rainier/Paradise Creek	08/12/10–09/11/12	Hourly	18 264	Cl^- flux	0.52	(0.22)
7	Rainier Nisqually River	10/15/10–09/18/12	Hourly	19 905	Cl^- flux	0.69	0.00
8	St. Helens/carbonate springs	08/18/09–08/04/12	Hourly	25 964	Cl^- flux	0.04	0.97
9	St. Helens/Kalama Spring	08/19/09–08/03/12	Hourly	27 864	Cl^- flux	0.95	0.00
11	Hood/Still Creek	07/16/09–09/12/12	Hourly	27 698	Cl^- flux	(0.35)	0.90
12	Austin Hot Springs	1984–2006	Intermittent	30	Cl^- flux[†]	0.30	(0.10)
		12/07/03–10/01/06	Bi-daily to hourly	4405	Cl^- flux[†]	0.20	0.04
13	Breitenbush Hot Sprs.	1984–2006	Intermittent	24	Cl^- flux[†]	0.13	(0.12)
14/15	McKenzie River	1984–2012	Intermittent	82	Cl^- flux[†]	0.25	(0.07)
16	South Sister/Separation Creek	2002–2004	4 daily to hourly	21 465	Cl^- flux	(0.28)	0.53
		2006–2012		37 169		0.09	0.10
17	South Sister/Mesa Creek	2002–2007	Bi-daily to hourly	5693	Cl^- flux[†]	(0.02)	0.66
		2008–2012		34 870		(0.21)	0.75
21	Shasta/Boles Creek	05/09/07–06/25/12	Hourly	44 992	Cl^- flux	0.92	0.00
23	Lassen/Manzanita Creek trib.	06/26/09–09/14/12	Hourly	28 220	HCO_3^- flux	0.94	0.14
24	Lassen/Devils Kitchen	1922–1996	Intermittent	15	Heat flux	0.93	(0.65)
		07/09/09–07/10/12	Hourly	17 616	Heat flux	0.71	(0.10)
25	Lassen/Mill Creek	1983–2012	Intermittent	48	Cl^- flux[†]	0.10	(0.10)

*Coefficient of determination (r^2) values for linear correlation; values in parenthesis indicate negative (inverse) correlation. [†]The chloride (Cl^-) flux values for these sites represent the hydrothermal component only; that is, the background Cl^- values upstream of the hydrothermal sources have been subtracted from the downstream Cl^- values (Fig. 4). Other Cl^- flux values are total fluxes.

gov/oa/documentlibrary/clim81supp3/tempnormal.pdf). We posit that a similar latitudinal variation exists west of the Rocky Mountains; however, western US air temperature records are also strongly influenced by orographic and ocean current effects, making it difficult to isolate latitudinal effects.

SEISMIC RESPONSE

Seismic monitoring is the backbone of volcano-monitoring efforts, and eruptions are nearly always preceded by increased seismicity. Thus, it is of interest to explore the sensitivity of the hydrothermal time series to seismic events.

A wide variety of hydrologic responses to earthquakes have been thoroughly discussed by Wang & Manga (2010), who suggest seismic energy density as a useful metric for purposes of comparison. The seismic energy density represents the maximum energy available in a seismic wave train to do work on a unit volume of rock ($J\ m^{-3}$) at a particular location, and can be empirically related to earthquake magnitude M and hypocenter distance r (Wang 2007):

$$log\ r = 0.48\ M - 0.33\ log\ e(r) - 1.4 \tag{1}$$

where e is the seismic energy density (hereinafter SED). The SED threshold has been shown to be approximately $0.001\ J\ m^{-3}$ for a variety of hydrothermal responses,
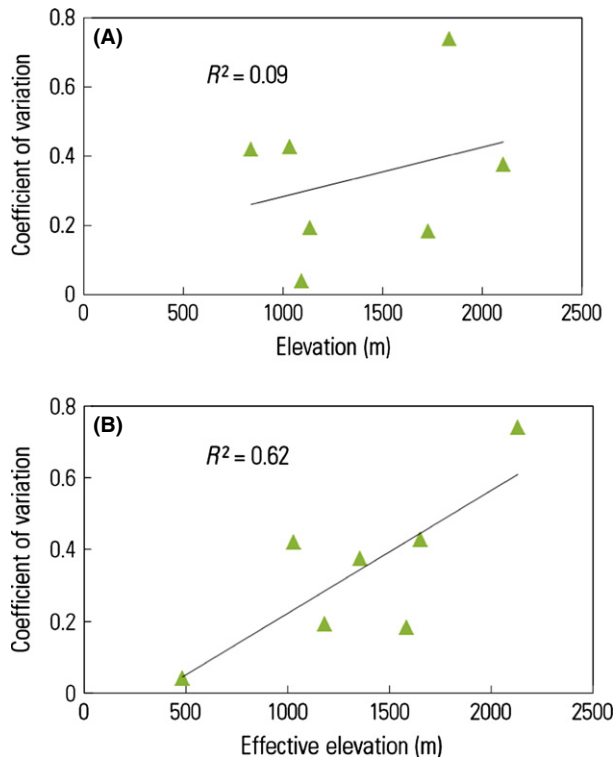
Fig. 12. Coefficient of variation (std. deviation/mean) of solute flux at smaller streams that capture outflow from nearby (≤400 m distant) springs with the evidence of magmatic influence (sites 3, 6, 9, 11, 17, 21, and 23 – see Fig. 10A) (A) as a function of site elevation and (B) as a function of 'effective' site elevation normalized to 45°N latitude under the assumptions discussed in the text.

namely changes in hot spring discharge (e.g., Sorey & Clark 1981), temperature in artesian geothermal wells (Mogi *et al.* 1989), and geyser frequency (e.g., Silver & Vallette-Silver 1992; Husen *et al.* 2004) (Fig. 13).

As of the end of the 2012 field season, there had been 87 occurrences of local SEDs approximately ≥ 0.001 J m^{-3} at our hourly recording hydrothermal-monitoring sites. The largest stimulus was approximately 0.01 J m^{-3} at carbonate springs, Mount St. Helens (site 8) on February 14, 2011. The great (*M* 9.0) Tohoku, Japan, earthquake of March 11, 2011, generated SED > 0.001 J m^{-3} at all 25 of the hydrothermal-monitoring sites.

There are many published examples of unambiguous hydrologic response to earthquakes (e.g., Wang & Manga 2010). Most of these occur either when one large earthquake simultaneously affects multiple discrete sites or when the response is sufficiently rare and large to be clearly attributed. For instance, the 1989 *M* 6.9 Loma Prieta earthquake in central California caused rapid (minutes to hours) and large (4–24-fold) increases in streamflow during a period of extended drought (Rojstaczer & Wolf 1992). The SEDs at the streams affected by the Loma Prieta event were relatively large, > 0.1 J m^{-3}.

We sorted the 87 occurrences of SED > 0.001 J m^{-3} in our records into two categories based on the visual inspection: 'no response' and 'possible response'. Responses labeled as 'possible' include the response of carbonate springs (Mount St. Helens, site 8) to the largest SED in our records (Fig. 14A) and the response of Mesa Creek
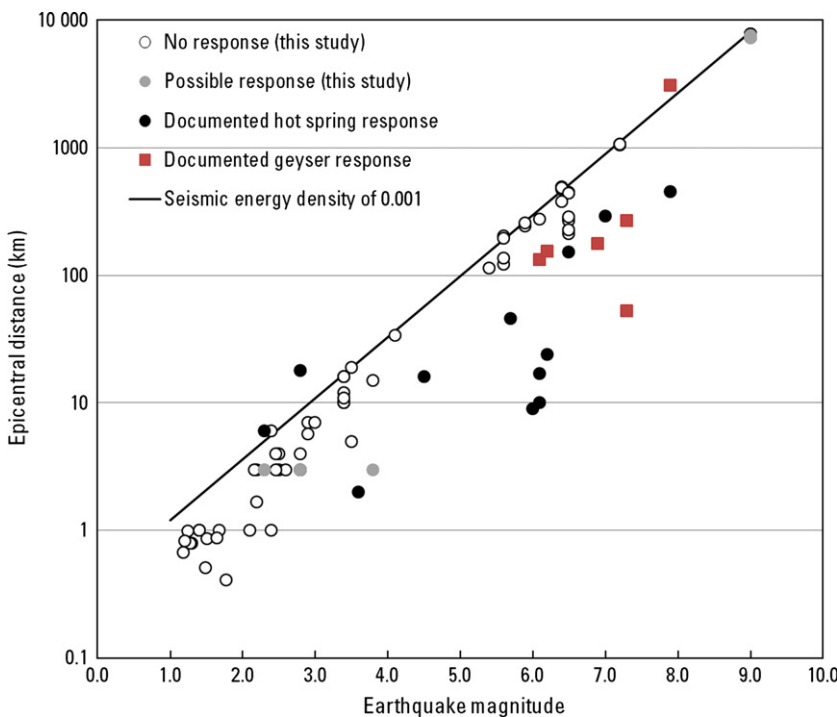

Fig. 13. Response of Cascade Range hydrothermal-monitoring sites to all seismic events that generated local seismic energy densities approximately ≥0.001 J m^{-3} during periods of hourly monitoring (*n* = 87). Documented (published) hot spring and geyser responses are from Sorey & Clark (1981), Silver & Vallette-Silver (1992), and the compilation by Wang & Manga (2010).
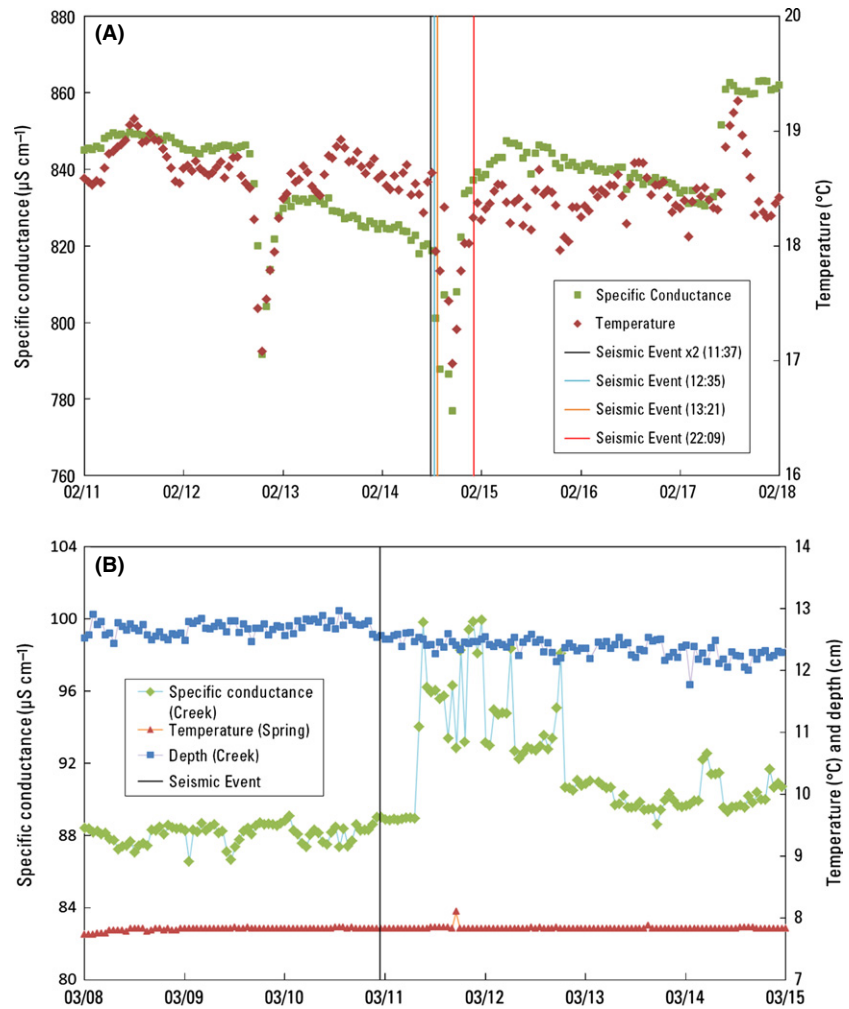
Fig. 14. Possible seismic responses of (A) carbonate springs (site 8) to four nearby M2.3–3.8 earthquakes on February 14, 2011 and (B) Mesa Creek and Mesa Spring (site 17) to a remote M9.0 earthquake at 22:46 PDT on March 10, 2011.

(South Sister, site 17) to the great Tohoku earthquake (Fig. 14B). These responses are not unambiguous. At carbonate springs (site 8), there is temporal correlation between the repeated seismic stimulus on 14 February and large changes in temperature and specific conductance (Fig. 14A); however, such large changes are not rare (see, e.g. 12 February). And whereas specific conductance in Mesa Creek and temperature in nearby Mesa Spring (Fig. 14B) increase following the Tohoku event, similar responses are not seen at any of the other sites, despite a nearly identical stimulus.

The 60-min recording interval adopted in this study – dictated by the limited storage capacity of the dataloggers and infrequent site visits – may not capture brief hydrogeologic responses. Nevertheless, results to date suggest that the Cascade Range hydrothermal-monitoring network is not highly sensitive to smaller SEDs in the range of 0.001–0.01 J m^{-3}. Earthquakes capable of generating SED $\gg$ 0.01 J m^{-3} are rare and did not occur during the 2009–2012 period when the network was fully deployed.

LONG-TERM TRENDS AT SELECTED SITES

Previous hydrothermal-monitoring studies in the western United States focused on distal, high-chloride springs and have shown these features to be quite stable over multidecadal periods of observation (Ingebritsen *et al.* 2001). The stability of distal, high-Cl^{-} hot springs is attributed to the longevity of the likely magmatic heat sources, flow path lengths ranging up to 10s of kilometers, and fluid travel times of perhaps 10^2–10^4 years.

This study focused instead on proximal features that exhibit clear evidence of magmatic input. What can be said about the multiyear to decadal term stability of these proximal features? Here, we consider the cases of South Sister, which inspired this hydrothermal-monitoring experiment; Mount St. Helens, where the hydrothermal system is still fast-evolving in response to the 1980–present eruptive cycle; and Lassen, where measurements taken in the early 1920s, shortly after the 1914–1917 eruptions, are compared with recent measurements.

South Sister – absence of clear trends 1990–present

The particulars of the South Sister hydrothermal anomaly were reviewed in the introduction of this paper, and its spatial relation to ongoing uplift and the March 2004 seismic swarm is shown in Fig. 2. Briefly, all helium–isotope ratios $>4R_A$ occur in springs with anomalous chloride, and many $^3He/^4He$ ratios near the center of the uplift are $>7R_A$, within the range found in mid-oceanic ridge basalt (MORB), which is typically given as 7–$9R_A$. These highly anomalous conditions clearly reflect the influence of magma. However, they may predate the onset of the ongoing (1996–1997 to present) uplift, as the total anomalous chloride flux in Separation Creek has remained indistinguishable from the initial value of 10 g s^{-1} measured in 1990 and reported by Ingebritsen *et al.* (1994).

Some subtle or localized hydrogeochemical changes may have been overlooked but, based on observations in hand, the magnitude and essential nature of the South Sister hydrothermal anomaly has not changed greatly between 1990 and 2012. A key characteristic of this anomaly is the intercorrelation among temperature, Cl$^-$ concentrations, and ^3He concentrations (Iverson 1999; Evans *et al.* 2002, 2004; van Soest *et al.* 2004). The hydrothermal Cl$^-$ flux in Separation Creek (site 16), which captures outflow from the entire anomaly, was 10 g s^{-1} in 1990 ($n = 1$), 10.0 ± 0.6 g s^{-1} in 2002–2004 ($n = 21\ 465$), and 10.3 ± 1.4 g s^{-1} in 2006–2012 ($n = 37\ 169$) (Table 1). Thus, there is no evidence of a significant change in Cl$^-$ flux associated with either the beginning of uplift in 1996–1997 or the earthquake swarm and slowing of uplift in 2004 (Fig. 15). There is a visible increase in the mean and variability of the Separation Creek Cl$^-$ flux during the final year of record (to 11.8 ± 1.75 g s^{-1} from June 26, 2011 to June 26, 2012) but, absent any corresponding change at Mesa Creek, we are loath to attribute causation. We note that the Separation Creek P-T-C probe was near the end of its design life by 2012, and had failed and was unresponsive by summer 2013. Both the Separation Creek and Mesa Creek records also exhibit some increase in variability in July 2008 that owes, at least in part, to the beginning of more frequent (hourly) recording at that time (Table 1).

The stability of the South Sister hydrothermal anomaly supports the tentative conclusion of Evans *et al.* (2004) that this anomaly might be related to frequent basaltic intrusion along north-trending lineaments on the west side of the Three Sisters. Evans *et al.* (2004) noted that intrusion of 0.006 km^3 year^{-1} of basaltic magma during five of every 100 years could sustain the present output of carbon, helium, and heat, and also maintain the distinctive magmatic gas signature of the springs. They further noted that no basalts have reached the surface in the Separation Creek drainage for at least 10 k.y. (Taylor *et al.* 1987) and that, viewed in this context, the intrusion inferred to cause the ongoing uplift has a low probability of actually erupting. Their conclusion was based on the hydrothermal data available through 2002. As of this writing, an additional decade of hydrothermal monitoring (Fig. 15) lends it further credence.

Mount St. Helens – secular trends at carbonate springs

The dynamic, fast-evolving nature of the post-1980 Mount St. Helens hydrothermal system poses its own unique opportunities and challenges for hydrothermal monitoring. Crandell & Mullineau (1978) recognized in the 1970s that Mount St. Helens is the most frequently active Cascade volcano, and it has erupted in 1980 and again in 2004. The USGS NVEWS report (Ewert *et al.* 2005) assigns Mount St. Helens the No. 1 threat score ranking among Cascade Range volcanoes.
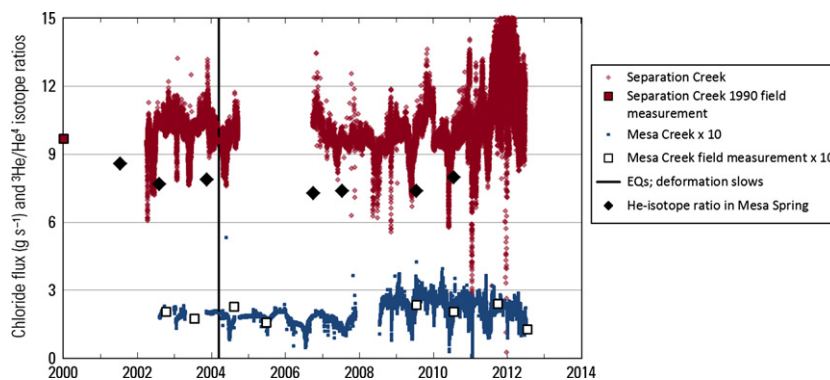

Fig. 15. Time series of chloride flux (g s^{-1}) in Mesa Creek (site 17) and Separation Creek (site 16) and $^3He/^4He$ isotope ratios in Mesa Spring. Peak geodetic uplift rates were 3–4 cm year^{-1} in 1998–2003, decreasing to 0.6–0.8 cm year^{-1} in 2006–2010; the change in inflation rate in approximately March 2004 (Riddick & Schmidt 2011; their Fig. 5) was roughly coincident with a swarm of approximately 300 small earthquakes (Moran 2004). The 1990 chloride flux measurement in Separation Creek clearly predates the beginning of uplift in 1996–1997. See Fig. 1 for hydrothermal-monitoring site locations and Fig. 2 for uplift pattern as of about 2002.

Observations prior to the 1980 eruption indicate that hydrothermal phenomena were weak and sparse. In 1941, surface temperatures of up to 88°C were measured at Boot Ridge, elevation 2740 m (Phillips 1941). In 1973–1974, temperatures of up to 89°C were measured at 50 cm depth on the southwest flank of Mt. St. Helens at approximately the same elevation (Friedman & Frank 1977). There were also unconfirmed reports of warm ground along the southern base of Pumice Butte on the Plains of Abraham, near the upper reaches (northern section) of the Ape Caves area, and near the terminus of the Floating Island Lava Flow, where sulfur fumes and elk licks were reported (Korosec et al. 1980).

The dynamic evolution of the post-1980 Mount St. Helens hydrothermal system can be briefly summarized as follows (Bergfeld et al. 2008): From the early 1980s to 2002, gas vents on the 1980–1986 dome grew weaker and more air-dominated. In the early 1980s, Loowit and Step hot springs emerged when canyons were eroded although the breach formed by the 1980 eruption (the 'Breach'). The highest water temperature recorded was 92.6°C from the Loowit spring group in 1986 (Shevenell & Goff 1993); subsequent declines in temperature and variable, but generally more dilute chemistry have been attributed to a rapidly cooling hydrothermal system. The Pumice Plain avalanche deposits lie below (north of) the Breach and below the Loowit and Step hot springs. Following brief fumarolic activity, thermal waters began to discharge from the cooling Pumice Plain deposits in 1981. The Pumice Plain thermal waters have cooled more rapidly than those along Loowit Creek and in Step Canyon; in general, the Pumice Plain thermal fluids seem to be confined to the shallow 1980 avalanche and pyroclastic deposits and do not contain magmatic volatiles. However, 'carbonate springs', (site 8) a large warm spring system on the northwest margin of the Pumice Plain, has chemical similarities to hot springs along Loowit Creek and in Step canyon.

Effort to develop continuous hydrothermal records from the Breach hot springs has been largely stymied by the aggressive water chemistry and an environment that remains unstable; multiple hot lahars occur in the Loowit and Step canyons every year. Instead, probes were installed in 'carbonate springs' (site 8), because of its chemical similarities to the Breach hot springs and evidence for magmatic carbon input (DIC >90% premodern C, δ^{13}C-DIC approximately −11), and in Kalama Spring (site 9), a large cold spring with minimal evidence of magmatic input which serves as a control.

The heat and solute output from Kalama Spring was steady during the 2009–2012 period of record (T = 4.0 ± 0.1°C, Cl⁻ flux 1.24 ± 0.52 g s⁻¹). In contrast, the 2009–2012 records from carbonate springs show substantial declines in heat and solute output (Fig. 16). The carbonate springs instrumental record is noisy, because there is significant conductivity drift and seasonal vegetation growth in the outflow channel. Nevertheless, the overall rates of decline indicated by the instrumental records and repeated field measurements are very similar.

The rapid decline in heat and solute flux seen at carbonate springs is similar to patterns observed in the mid-valley thermal springs in Valley of 10 000 Smokes, Alaska, where heat discharges from a still-cooling 1912 ashflow sheet (e.g., Hogeweg et al. 2005). The inference in both cases is that heat and solutes are being mined from a source that is relatively local, shallow, and transient.

Lassen – comparison of measurements in early 1920s, 1970s, 1990s, and 2009–2012

The Lassen volcanic center hosts the largest and most visible high-temperature hydrothermal system in the Cascade Range. Most of the obvious hydrothermal activity is south and southeast of Lassen Peak, where the detection of any possible magmatic signature in surface features is complicated by boiling and phase separation associated with an underlying vapor-dominated zone (or zones). Thus, two of the three Lassen sites selected for continuous hydrogeochemical monitoring are north of Lassen Peak (sites 22 and 23). The exception is Devils Kitchen (site 24), one of several major areas of fumarolic discharge, where hourly heat flow measurements were taken in 2009–2012.

The Devils Kitchen fumarolic area was selected for continuous monitoring for two reasons: (i) there is an unusually long record of heat flow measurement, and (ii) the dominant component of heat flow is readily measured. Measurements of heat flow at Devils Kitchen were first taken in 1922–1923 (Day & Allen 1925), shortly after the 1914–1917 Lassen Peak eruption, and intermittent measurements were taken from 1974 to 1996 (Friedman & Frank 1978; Sorey & Colvard 1994; Ingebritsen et al. 2001). Further, whereas measurement of heat flow from fumarolic areas is usually difficult and time-consuming, the dominant mode of heat loss from Devils Kitchen is straightforward to measure.

In general, significant heat loss from fumarolic areas occurs by direct discharge from fumaroles (H_{FUM}); by direct discharge from hot springs (H_{HS}) and lateral seepage in the subsurface (H_{LAT}); by evaporation and radiation from water surfaces (H_{WS}); by conduction, advection, and evaporation from hot ground (H_{GR}); and by advection in streams (H_{ADV}). That is,

$$H_{TOT} = H_{FUM} + H_{HS} + H_{LAT} + H_{WS} + H_{GR} + H_{ADV} \quad (2)$$

where (H_{TOT}) is the total heat loss from the thermal area. Measurement of these multiple modes of heat discharge is difficult, and most of these terms are also model-dependent. Thus, the uncertainties are large, and time series are sparse and rare – both in the Cascade Range and globally.
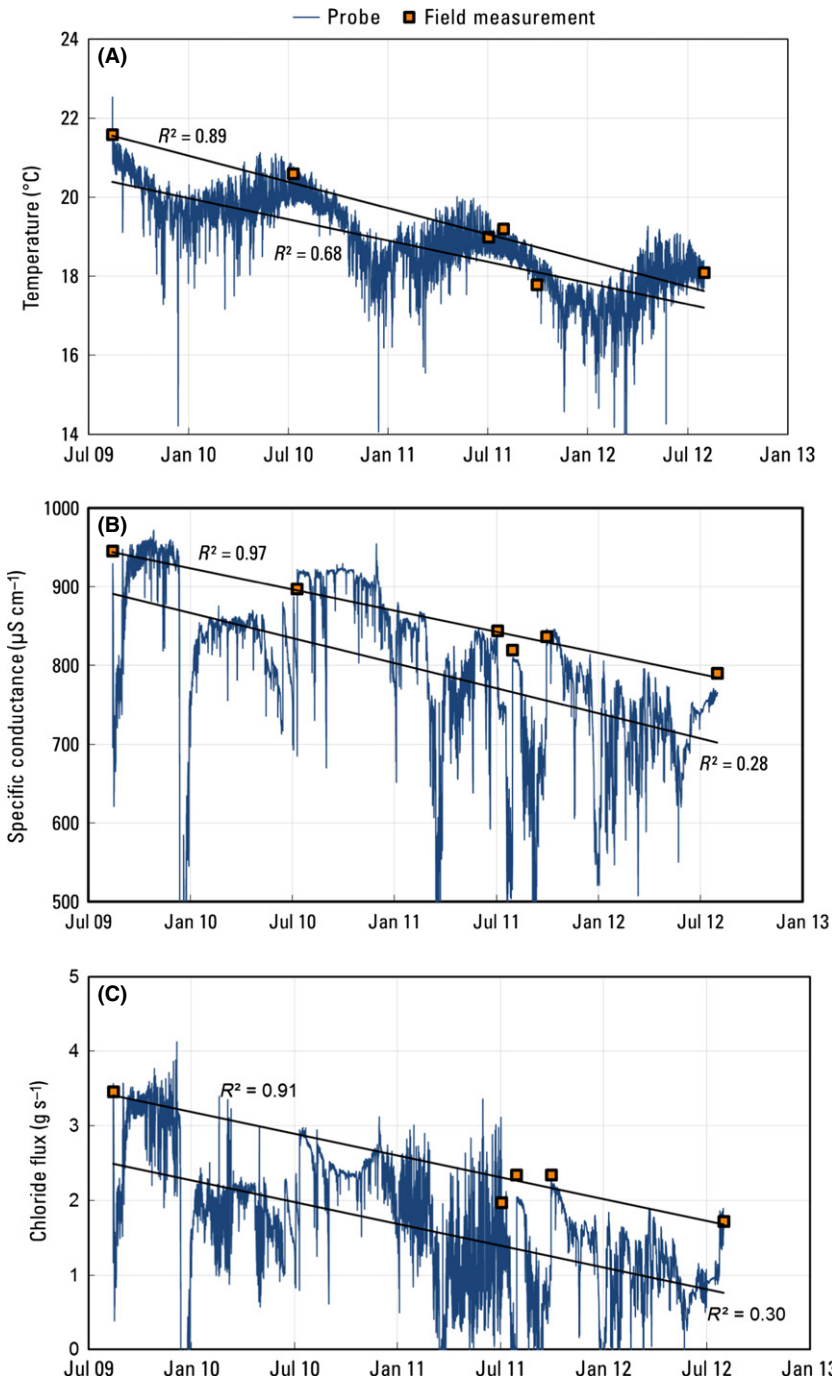
Fig. 16. Temporal trends in (A) temperature, (B) specific conductance, and (C) chloride flux at carbonate springs, Mount St. Helens (site 8). In each panel, the upper trend line is fit to field measurements, the lower trend line to probe data.

However, based on measurements by Sorey & Colvard (1994) in 1986–1993, Hot Springs Creek advects about half ($H_{ADV} = 10.4 \pm 2.7$ MW) of the heat from Devils Kitchen ($H_{TOT} = 21 \pm 4$ MW). Heat advected by Hot Springs Creek (H_{ADV}) is readily calculated as

$$H_{ADV} = Q_{DS}(T_{DS} - T_{US}) \qquad (3)$$

where Q_{DS} is the discharge of Hot Springs Creek downstream, T_{US} is the stream temperature upstream of the hydrothermal area, and T_{DS} is the stream temperature downstream. To measure this quantity, P-T-C probes were installed upstream and downstream of Devils Kitchen from June 24, 2009 to July 10, 2012.

What do the cumulative 1922–2012 records suggest about the presence or absence of long-term trends? The hourly records from 2009 to 2012 show heat advected in Hot Springs Creek (H_{ADV}) ranging from approximately 5–25 MW (mean 13.5 MW) (Fig. 17), with the variation controlled largely by stream discharge (Table 3: $r^2 = 0.71$). The P-T-C hourly records can also be used to estimate total heat

loss (H_{TOT}), because steam contributes both sulfur and heat to Hot Springs Creek. Assuming that all of the H_2S associated with the steam eventually converts to SO_4^{2-} and is swept downstream, then the average SO_4^{2-} output from Devils Kitchen (approximately 5 g s^{-1}) can be multiplied by the known mass ratio of steam/H_2S (approximately 1400, Janik & McLaren 2010) and the enthalpy of steam (2800 kJ kg^{-1}) to obtain a sulfate-flux-based estimate of H_{TOT}. The resulting SO_4^{2-}-flux-based estimate of H_{TOT} in 2010–2012 is approximately 20 MW, very similar to the value measured by Sorey & Colvard (1994) in 1986–1993 using other methods (Eq. 2). Native sulfur and pyrite (FeS_2) are both commonly visible at Devils Kitchen and represent local, temporary storage of sulfur at intermediate oxidation states. However, the near-zero SO_4^{2-} fluxes observed for brief periods in late spring 2011 and 2012 (Fig. 17) suggest that these surficial S-storage reservoirs may empty seasonally.

The entire 1922–2012 Devils Kitchen heat flow record exhibits internal consistency. Observed variation in heat flow from 1922 to 1996 ($n = 15$) relates mainly to variations in stream discharge (Ingebritsen et al. 2001; their Fig. 8); this is also the case for the much higher-resolution 2010–2012 record ($n = 17\,626$). Further, maximum measured heat flow values from the early 1920s (26 MW, $n = 2$) are no larger than the maximum values measured in 2010–2012 (Fig. 17: 25–30 MW). Finally, in 2010–2012, both heat advection in Hot Springs Creek ($H_{ADV} = 10.9$ MW) and total heat loss based on SO_4^{2-} flux (H_{TOT} approximately 20 MW) were similar to the H_{ADV} and H_{TOT} values measured in 1986–1993 by Sorey & Colvard (1994) (10.4 and 21 MW, respectively, for a much smaller sample size).

There are at least two possible explanations for the apparent stability of Devils Kitchen heat flow from the early 1920s to present. First, the hydrothermal system may have been restored to near-equilibrium conditions within 5 years of the 1914–1917 eruption. Alternatively, the major fumarolic areas of Lassen system may not have responded dramatically to the 1914–1917 eruption. If so,
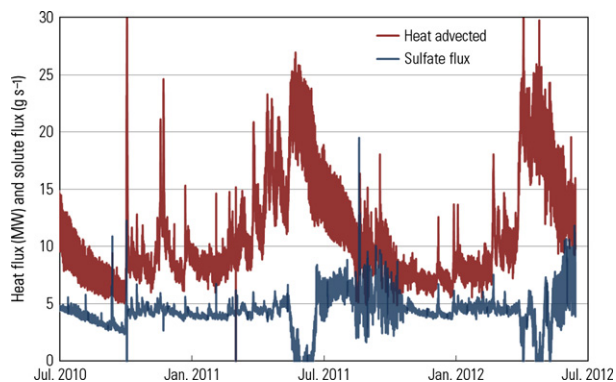
their lack of response may relate to the unusual buffering capacity of extensive two-phase zones, which possess very high effective compressibility (Grant & Sorey 1979; Ingebritsen & Sorey 1985). The latter possibility supports the selection of hydrothermal-monitoring sites north of Lassen Peak that avoid the extensive two-phase zone(s).

DISCUSSION AND FUTURE DIRECTIONS

The Cascade Range is a relatively quiescent volcanic arc. Eruptions have occurred an average of every 50 years over the past 4000 years (Dzurisin et al. 1997). This prehistoric rate is compatible with the approximately 200-year historical record of two eruptions (Lassen 1914–1917 and Mount St. Helens 1980–present) and two well-documented 'failed eruptions' (Mount Baker 1975 and South Sister 1996–present). Thus, the statistical likelihood of capturing a Cascade Range eruptive cycle during a several-year period of hydrothermal monitoring is rather low.

One advantage of carrying out the hydrothermal-monitoring experiment in this relatively quiescent volcanic arc is ease-of-access. In the Cascades, it is logistically feasible to simultaneously occupy the most promising hydrothermal-monitoring sites arc-wide. This would not be the case in the more active but less accessible Aleutian arc.

The Cascade Range data also serve to establish a baseline for campaign-style response to future episodes of volcanic unrest. Consider for instance Mount Baker (Fig. 1). Other than the fumarolic areas in Sherman Crater (site 1; see Werner et al. 2009), the Sulphur Creek tributary (site 3) is the most obvious target for hydrothermal monitoring, because of its chloride content and magmatic carbon signature (>90% premodern C). (Boulder Creek – site 2 – which drains Sherman crater, is another obvious monitoring target but lacks a deep hydrothermal signature.) Yet Sulphur Creek exhibits a 5–10-fold variation in solute flux (Cl$^-$ flux 0.3–2.8 g s^{-1}) due to purely hydrologic factors (Fig. 5C). In the absence of year-round baseline data, the results of campaign-style sampling of Sulphur Creek would be very difficult to interpret; clearly, a large change in Cl$^-$ flux might be purely hydrologic. In contrast, any measurable change in Cl$^-$ flux at Boles Creek (Mount Shasta, site 21), where changes in Cl$^-$ flux were essentially undetectable in 2007–2012 (0.149 ± 0.006 g s^{-1}), might be of real interest.

Experience gained in the Cascade Range documents the potential importance of year-round monitoring, as well as the importance of sufficiently high temporal resolution to document diurnal variability and assess seismic responses. Cascades Range experience also suggests that persistent anomalies, such as those at South Sister, may reveal the locations of frequent 'failed eruptions' (e.g., dike intrusions) and that extensive two-phase zones, such as those at Lassen, might tend to mask signals from depth. Future work on the Cascade Range database will include detailed

Fig. 17. Two-year time series of heat and sulfate flux in Hot Springs Creek immediately downstream of Devils Kitchen, Lassen Volcanic National Park (site 24).

time-series analysis, including spectral and wavelet analysis. Filtering of periodicities in the time series that are related to near-surface forcing may enhance the ability to detect potential variations associated with processes at depth.

We continue to believe that geochemical changes in magmatically influenced springs on the flanks of volcanoes may prove to be of diagnostic value. The ^{3}He/^{4}He ratio seems to be the best single geochemical indicator of magmatic influence (e.g., Sorey *et al.* 1998), and at times ^{3}He/^{4}He ratios have been observed to be higher in selected flank springs than in summit fumaroles, for instance at Mount Hood in the 1990s and Mount Shasta in the 2000s (Ingebritsen *et al.* 2014).

Future hydrothermal monitoring will focus on more active volcanoes, in an effort to continuously monitor hydrothermal phenomena through full cycles of volcanic unrest, and on more direct sampling of the hydrogeochemical parameters believed to be of most interest. In a US context, the emphasis on capturing full volcanic-unrest cycles implies increased focus on the Alaskan/Aleutian arc, where eruptions are much more common (often > 1 per year, versus 1/50 years in the Cascades), and on eastern California, where signs of volcanic unrest ('failed eruptions') are relatively common. We are also experimenting with ways to directly and continuously sample gas composition and particularly the ^{3}He/^{4}He ratio. To this end, the University of Utah Noble Gas Laboratory has developed a suite of passive diffusion samplers (Gardner & Solomon 2009) with a wide range of nominal mean equilibration times (hours to months). These devices can be left in place indefinitely, either in hot ground or in magmatically influenced springs, and retrieved in response to independent geophysical signals of volcanic unrest. Inherent design features are that the stored sample evolves continuously to reflect local *in situ* conditions and that inverse methods can be used to infer the timing and magnitude of any gas composition changes. In collaboration with the University of Utah and the Geological Survey of Japan, prototype devices have been tested in the Cascade Range (sites 8, 19, and 23) and are currently (spring 2013 to present) deployed at the restless Izu-Oshima volcano, Japan.

ACKNOWLEDGEMENTS

REFERENCES

Barringer JW, Johnsson PA (1996) Theoretical considerations and a simple method for measuring alkalinity in low-pH waters by Gran titration: U.S. Geological Survey Water-Resources Investigations Report 89-4029, 36.

Bergfeld D, Evans WC, McGee KA, Spicer KR (2008) Pre- and post-eruptive investigations of gas and water samples from Mount St. Helens, Washington, 2002 to 2005. In: *A Volcano Rekindled: The Renewed Eruption of Mount St. Helens, 2004–2006* (eds Sherrod DR, Scott WE, Stauffer PH), pp. 523–42. U.S. Geological Survey Professional Paper 1750, Reston, VA.

Chiodini G, Brombach T, Caliro S, Cardellini C, Marini L, Dietrich V (2002) Geochemical indicators of possible ongoing volcanic unrest at Nisyros Island (Greece). *Geophysical Research Letters*, **29**, 6-1–6-4. doi:10.1029/2001GL014355

Connor CB, Clement BM, Song X, Lane SB, West-Thomas J (1993) Continuous monitoring of high-temperature fumaroles on an active lava dome, Volcan Colima, Mexico: evidence of mass flow variation in response to atmospheric forcing. *Journal of Geophysical Research*, **98**, 19713–22.

Crandell DR, Mullineau DR (1978) Potential hazards from future eruptions of Mount St. Helens volcano, Washington. *U.S. Geological Survey Bulletin*, **1383-C**, 26.

Day AL, Allen ET (1925) The volcanic activity and hot springs of Lassen Peak. Carnegie Institution of Washington Publication 390, pp. 190.

Dzurisin D, Stauffer PH, Hendley JW II (1997) Living with volcanic risk in the Cascades. U.S. Geological Survey Fact Sheet 165-97, pp. 2. (Revised March 2008)

Ellis AJ, Wilson SH (1955) The heat from the Wairakei-Taupo thermal region calculated from the chloride output. *New Zealand Journal of Science and Technology B, General Research Section*, **36**, 622–31.

Evans WC, Banks NG, White LD (1981) Analyses of gas samples from the summit crater. In: *The 1980 eruptions of Mount St. Helens, Washington* (eds Lipman PW, Mullineaux DR), pp. 227–32. U.S. Geological Survey Professional Paper 1250, Washington, DC.

Evans WC, Mariner RH, Ingebritsen SE, Kennedy BM, van Soest MC, Huebner MA (2002) Report of hydrologic investigations in the Three Sisters area of central Oregon, summer 2001. U.S. Geological Survey Water-Resources Investigations Report 02-4061, pp. 13. http://water.usgs.gov/pubs/wri/wri024061.

Evans WC, van Soest MC, Mariner RH, Hurwitz S, Ingebritsen SE, Wicks CW Jr, Schmidt ME (2004) Magmatic intrusion west of Three Sisters, central Oregon, USA: the perspective from spring geochemistry. *Geology*, **32**, 69–72.

Ewert JW, Guffanti M, Murray TL (2005) An assessment of volcanic threat and monitoring capabilities in the United States:

Framework for a National Volcanic Early Warning System. U.S. Geological Survey Open-File Report 2005-1164, pp. 62.

Friedman JD, Frank D (1977) Thermal surveillance of active volcanoes using the Landsat-1 data collection systems – Part III – Heat discharge from Mount St. Helens, Washington. U.S. Geological Survey Open-File Report 77-541, pp. 28.

Friedman JD, Frank D (1978) Thermal surveillance of active volcanoes using the Landsat-1 data collection system. National Technical Information Services Report NTIS N78 23499/LL, pp. 46.

Gardner P, Solomon DK (2009) An advanced passive diffusion sampler for the determination of dissolved gas concentrations. *Water Resources Research*, **45**, W06423.

Gottsmann J, Folch A, Rymer H (2006) Unrest at Campi Flegrei: a contribution to the magmatic versus hydrothermal debate from inverse and finite element modeling. *Journal of Geophysical Research*, **111**, B07203.

Gottsmann J, Carniel R, Coppo N, Wooller L, Hautman S, Rymer H (2007) Oscillations in hydrothermal systems as a source of periodic unrest at caldera volcanoes: multiparameter insights from Nisyros, Greece. *Geophysical Research Letters*, **34**, L07307.

Grant MA, Sorey ML (1979) The compressibility and hydraulic diffusivity of a water-steam flow. *Water Resources Research*, **15**, 684–6.

Hiyagon H, Kennedy BM (1992) Noble gases in CH_4-rich gas fields, Alberta, Canada. *Geochimica et Cosmochimica Acta*, **56**, 1569–89.

Hochstein MP, Bromley CJ (2005) Measurement of heat flux from steaming ground. *Geothermics*, **34**, 133–60.

Hogeweg N, Keith TEC, Colvard EM, Ingebritsen SE (2005) Ongoing hydrothermal heat loss from the Valley of 10,000 Smokes, Alaska. *Journal of Volcanology and Geothermal Research*, **143**, 279–91.

Husen S, Taylor R, Smith RB, Heasler H (2004) Changes in geyser eruption behavior and remotely triggered seismicity in Yellowstone National Park induced by the 2002 M7.9 Denali fault earthquake. *Geology*, **32**, 537–40.

Ingebritsen SE, Sorey ML (1985) A quantitative analysis of the Lassen hydrothermal system, north central California. *Water Resources Research*, **21**, 853–68.

Ingebritsen SE, Mariner RH, Sherrod DR (1994) Hydrothermal systems of the Cascade Range, north-central Oregon. U.S. Geological Survey Professional Paper 1044-L, pp. 86, 2 plates.

Ingebritsen SE, Galloway DL, Colvard EM, Sorey ML, Mariner RH (2001) Time-variation of hydrothermal discharge at selected sites in the western United States: implications for monitoring. *Journal of Volcanology and Geothermal Research*, **111**, 1–23.

Ingebritsen SE, Gelwick KD, Randolph-Flagg NG, Crankshaw IM, Lundstrom EA, McCulloch CL, Murveit AM, Newman AC, Mariner RH, Bergfeld D, Tucker DS, Schmidt ME, Spicer KR, Mosbrucker A, Evans WC (2014) Hydrothermal monitoring data from the Cascade Range, northwestern United States. U.S. Geological Survey Data Set, doi:10.5066/F72N5088, http://water.usgs.gov/nrp/cascade-hydrothermal-monitoring/.

Iverson JT (1999) An investigation of the chloride anomaly in Separation Creek, Lane County, Oregon. Unpublished senior honors thesis, Oregon State University, Corvallis, pp. 61.

Janik CJ, McLaren MK (2010) Seismicity and fluid geochemistry at Lassen Volcanic National Park, California: evidence for two circulation cells in the hydrothermal system. *Journal of Volcanology and Geothermal Research*, **189**, 257–77.

Kennedy BM, Lynch MA, Reynolds JH, Smith SP (1985) Intensive sampling of noble gases in fluids at Yellowstone: early

overview of the data, regional patterns. *Geochimica et Cosmochimica Acta*, **49**, 1251–61.

Korosec MA, Schuster JE, with contributions by Blackwell DD, Zanes ZF, Clayton GA (1980) The 1979-1980 geothermal resource assessment program in Washington. Washington Division of Geology and Earth Resources Open-File Report 81-3, 148 p. + appendices + 1 plate.

Manga M (1996) Hydrology of spring-dominated streams in the Oregon Cascades. *Water Resources Research*, **32**, 2435–9.

Manga M (1997) A model for discharge in spring-dominated streams and implications for the transmissivity and recharge of Quaternary volcanics in the Oregon Cascades. *Water Resources Research*, **33**, 1813–22.

Mogi K, Mochizuki H, Kurokawa Y (1989) Temperature changes in an artesian spring at Usami in the Izu Peninsula (Japan) and their relation to earthquakes. *Tectonophysics*, **159**, 95–108.

Moran SC (2004) Seismic monitoring at Cascade volcanic centers, 2004: Status and recommendations. U.S. Geological Survey Scientific Investigations Report 2004-5211, pp. 22.

Muffler LJP, Nehring NL, Truesdell AH, Janik CJ, Clynne MA, Thompson JM (1982) The Lassen geothermal system: U.S. Geological Survey Open-File Report 82-926, pp. 8. Also published in the Proceedings of the Pacific Geothermal Conference, Auckland, New Zealand, November 1982.

Nolan KM, Shields RR (2000) Measurement of stream discharge by wading. U.S. Geological Survey Water-Resources Investigations Report 00-4036, http://wwwrcamnl.wr.usgs.gov/sws/SWTraining/WRIR004036/Index.html.

Padron E, Perez NM, Hernandez PA, Sumino H, Melian GV, Barrancos J, Nolasco D, Padilla G, Dionis S, Rodriguez F, Hernandez I, Calvo D, Peraza MD, Nagao K (2013) Diffusive helium emissions as a precursory sign of volcanic unrest. *Geology*, **41**, 539–42.

Phillips KN (1941) Fumaroles of Mount St. Helens and Mount Adams. *Mazama*, **23**, 37–42.

Riddick SN, Schmidt DA (2011) Time-dependent changes in volcanic inflation rate near Three Sisters, Oregon, revealed by InSAR. *Geochemistry Geophysics Geosystems*, **12**, Q12005.

Rojstaczer S, Wolf S (1992) Permeability changes associated with large earthquakes: an example from Loma Prieta, California. *Geology*, **20**, 211–4.

Shevenell L, Goff F (1993) Addition of magmatic volatiles into the hot spring waters of Loowit Canyon, Mount St. Helens, Washington, USA. *Bulletin of Volcanology*, **55**, 489–503.

Silver PG, Vallette-Silver NJ (1992) Detection of hydrothermal precursors to large northern California earthquakes. *Science*, **257**, 1363–8.

van Soest MC, Evans WC, Mariner RH, Schmidt ME (2004) Chloride in hot springs of the Cascade volcanic arc – The source puzzle. In: *Proceedings of the Eleventh International Symposium on Water-Rock Interaction, June 27-July 2, 2004* (eds Wanty RB, Seal RR II), pp. 209–13. Taylor and Francis, Saratoga Springs, NY.

Sorey ML, Clark MD (1981) Changes in the discharge characteristics of thermal springs and fumaroles in the Long Valley caldera, California, resulting from earthquakes on May 25–27, 1980. U.S. Geological Survey Open-File Report 81-203, pp. 22.

Sorey ML, Colvard EM (1994) Measurements of heat and mass flow from thermal areas in Lassen Volcanic National Park, California, 1984–93. U.S. Geological Survey Water-Resources Investigations Report 94-4180-A, pp. 35.

Sorey ML, Evans WC, Kennedy BM, Farrar CD, Hainsworth LJ, Hausback B (1998) Carbon dioxide and helium emissions from

a reservoir of magmatic gas beneath Mammoth Mountain, California. *Journal of Geophysical Research*, **103**, 15303–23.

Taylor EM, MacLeod NS, Sherrod DR, Walker GW (1987) Geologic map of the Three Sisters Wilderness, Deschutes, Lane, and Linn Counties, Oregon. U.S. Geological Survey Miscellaneous Field Studies Map MF-1952, scale 1:63,360.

Tedesco D (1994) Chemical and isotopic gas emissions at Campi Flegrei: evidence for an aborted period of unrest. *Journal of Geophysical Research*, **99**, 15623–31.

Todesco M (2008) Hydrothermal circulation and its effect on caldera unrest. *Developments in Volcanology*, **10**, 393–416.

Todesco M, Rinaldi AP, Bonafede M (2010) Modeling of unrest signals in heterogeneous hydrothermal systems. *Journal of Geophysical Research*, **115**, B09213.

Wang C-Y (2007) Liquefaction beyond the near field. *Seismological Research Letters*, **78**, 512–7.

Wang C-Y, Manga M (2010) *Earthquakes and Water*. Springer-Verlag, Berlin Heidelberg, pp. 225. (Lecture Notes in Earth Sciences 114)

Werner C, Evans WC, Poland M, Tucker DS, Doukas MP (2009) Long-term changes in quiescent degassing at Mount Baker volcano, Washington: evidence for a stalled intrusion in 1975 and connection to a deep magma source. *Journal of Volcanology and Geothermal Research*, **186**, 379–86.

Wicks CW Jr, Dzurisin D, Ingebritsen SE, Thatcher W, Lu Z, Iverson J (2002) Magmatic activity beneath the quiescent Three Sisters volcanic center, central Oregon Cascade Range, Oregon. *Geophysical Research Letters*, **29**, 1122.

GEOFLUIDS

CONTENTS